Coupled Oscillators for Orientation Dynamics

Author:
Lamees Felemban
Supervisor:
Jan Sieber

University of Exeter

Submitted by Lamees Felemban, to the University of Exeter as a dissertation for the degree of **Masters by Research in Mathematics** in March 2019.

I certify that all material in this dissertation which is not my own work has been identified and that any material that has previously been submitted and approved for the award of a degree by this or any other University has been acknowledged.

I would like to dedicate this thesis to the warriors who never gave up their fight against anxiety and/or depression despite those judging and underestimating their ongoing battles

Declaration

I hereby declare that except where specific reference is made to the work of others, the contents of this dissertation are original and have not been submitted in whole or in part for consideration for any other degree or qualification in this, or any other university. This dissertation is my own work and contains nothing which is the outcome of work done in collaboration with others, except as specified in the text and Acknowledgements. This dissertation contains fewer than 65,000 words including appendices, bibliography, footnotes, tables and equations and has fewer than 150 figures.

Author:
Lamees Felemban
Supervisor:
Jan Sieber
November 2019

Acknowledgements

First and foremost I would like to thank Allah for providing me with everything that made accomplishing this thesis possible. I would also like to thank my supervisor Jan Sieber, for guiding me through my journey to accomplish this thesis. He's been informative and patient. I would also like to offer my thanks to my office colleagues Courtney Quinn, Damian Smug, Paul Ritchie, Swinda Falkena and Hassan Alkhayuon for many interesting discussion.

I would like to acknowledge the rest of my office colleagues Abdullah, Tomas, Burhan and Saad who made working at the University of Exeter an unforgettable experience. To Dina and Claudia my friends from the University who also happened to be my neighbours for all the support. Finally, I would like to thank my parents for giving me everything including financial support before I joined the scholarship program offered by Saudi cultural bureau on my second year. My friends Abrar, Ashymaa and Helen who never gave up on me. My professor from KAU who helped me discover what I am capable of. Lastly to the teacher who taught me how to read and write.

Abstract

In this thesis we study a system of coupled phase oscillators that models animals group decision making for direction of travel. Each oscillator is an individual and its phase represents the orientation of the individual. We study the scenario where some individuals have preferred directions. Since the model has a gradient structure we can exclude oscillatory solutions. We also show that in stable equilibria individuals with the same preferred direction and preference strength must have identical orientation if the coupling between oscillators is harmonic. An arbitrarily small perturbation of harmonic coupling may lead to a split of groups with identical preferences. We produce bifurcation diagrams for the case where the population consists of three groups: two groups with conflicting preferred directions and one group without preference. We locate symmetry breaking points branches of equilibria and observe different bistability regions for three different values of the coupling coefficients: weak, moderate and strong.

Table of contents

List of figures

Chapter 1

Introduction

The scene of fireflies population firing harmoniously is so beautiful that people may choose to watch it in the forest over city luxurious entertainment during the weekend. Luckily among these people there are scientists who are able to find out the mathematics hidden behind this beautiful harmonious scene in nature. Also these scientists would devote their lives to reveal the secret of nature's beauty to all mankind. While watching fireflies a scientist may wonder how is it possible that fireflies synchronise given that initially each firefly was firing with different frequency. A remarkable scientist named Kuramoto came up with a mathematical model that idealizes the problem of coupled self-sustained oscillators such as the firing of fireflies (see the review by Acebrón et al. [1]). He noted that for synchronization the important quantities are the natural frequency ω_i and the phase $\phi_i(t)$ of each oscillator i. The mathematical model assumes that the time derivative of an oscillator phase is equal to its natural frequency ω_i plus the averaged phase difference between oscillator i and all other oscillators that belong to the same population. The simplest model has the following formula

$$\dot{\phi}_i = \omega_i + \frac{1}{N}\sum_{j=1}^{N} K_{ij}\sin(\phi_j - \phi_i). \quad \text{for} \quad i = 1, ..., N \tag{1.1}$$

where ω_i is the natural frequency of the oscillator and K_{ij} is the coupling coefficient between oscillators i and j. Other examples of systems that are modelled by phase oscillators are neurons [8]. For further reading about the model see Strogatz [22], Jadbabaie et al. [12], Acebrón et al. [1], Mirollo and Strogatz [18].

The study of animal coordination decision making in large flocks is a topic that has been addressed with models that look similar to the classical Kuramoto

oscillator network (1.1). An idealized scenario is that a flock consists of a large number individuals who all follow simple *social interaction forces* such as collision avoidance and attraction to other individuals. A decision making problem for the flock occurs if some (at least two) small subgroups of individuals possess additional information, for example, about food sources or predators. Now each individual in each of these subgroups is subject to an additional *bias* force representing this additional information, pulling in possibly different directions. Depending on the overall balance of bias and social forces for each individual in the flock, the flow may follow the preference of either of the subgroups or it may split. There is a delicate balance between the benefits of reacting rapidly to information by subgroups and of the flock staying together. The dynamics caused by this balance was explored in theoretical ecology using mathematical models [4, 5, 11]. Couzin and Franks [4] observed decision making for fish to join a group(shoaling) in response to changes in environmental conditions or internal state. Hoare et al. [11] showed how a collective choice of direction is made in a population of ants under the impact of individual ants movements on trails. Couzin et al. [5] analysed the balance between splitting and speed of decision making. We provide more details about this in section 1.2. One important quantity for individuals in animal groups (such as fish schools or ant population) is its orientation. This orientation would also be described as a phase angle ϕ if the motion is in the plane. If one ignores the effects of position (as more idealized models by Leonard et al. [16], Nabet et al. [21] do), the dynamics of the individuals' orientations is also described by coupled phase oscillators. An important difference is, however, that instead of a natural frequency ω_i individuals may have a preferred orientation $\bar{\phi}_i$ and some strength of preference a_i. This preference models the *bias*, for example, of the form $a_i \sin(\bar{\phi}_i - \phi_i)$ that replaces the natural frequency ω_i in (1.1). The preferred orientation encodes the knowledge of the individual about food sources or predators. Studies by Couzin et al. [5], Leonard et al. [16] or Nabet et al. [21] have created and analysed a hierarchy of models for decision making if only some individuals have a preference and most individuals follow only the coupling forces (the so-called social interaction forces).

Motivated by the result in Couzin et al. [5] on the splitting of groups, we focus on the question if it is possible that the group of individuals with no preference (the *naive* group) splits in the model proposed by Nabet et al. [20], which considers only the orientation of each individual and uniform global coupling, resulting in a fully coupled network of individuals represented by phases.

This thesis analyses the model by Nabet et al. [20] in more detail and obtains the following new mathematical results. We prove that with purely sinusoidal coupling between individuals with the same preference will always align asymptotically. In particular, this implies that the naive group (the individuals with no bias) will *not* split. We formulate this as a theorem and give a rigorous proof in Chapter 2. We also demonstrate that arbitrarily small perturbations to sinusoidal coupling will permit scenarios where the naive group can split. We prove that this split occurs when one has two large informed groups with nearly opposite preferences and the naive group is relatively small. For the limit of strong coupling we provide a singular perturbation analysis that reduces the large network to a single differential equation. This is a correction to the incomplete singular perturbation analysis by Nabet [19].

In chapter three we perform a numerical bifurcation analysis for the case of three groups introduced by Nabet et al. [20]: two small groups of equal size with different preferred directions and one larger group with no preference, which is the scenario considered by Leonard et al. [16]. We study the dependence of group orientations in stable equilibria on two parameters: the difference between preferred directons of the informed groups, denoted by $\bar{\theta}_1 - \bar{\theta}_2$, and the uniform coupling strength K which is a parameter that was not considered by Leonard et al. [16]. While Nabet *et al* [20, 19] provide explicit formulas to the location of equilibria for some cases, our bifurcation diagrams give the systematic picture: for all coupling strengths there exists a region of bistability $\bar{\theta}_1 - \bar{\theta}_2$ near π (that is, when the informed groups have diametrically opposing preferences). The region of bistability is largest for intermediate coupling strengths K but shrinks for large and small (positive) K. We illustrate the resulting stable orientation configurations from branches of equilibria, presenting them graphically. This systematic overview is also a novel result of this thesis.

The following subsections of the introduction review some uses of phase oscillators in the literature. We start with a case where phase oscillators were used for studying synchronization of rhythmic motion (fireflies falshing) by Ermentrout [8]. In section 1.2 we first summarize the results for a detailed flock model by Couzin et al. [5] where phases represent orientations. Then we move on to gradually more idealized models by Leonard et al. [16] and Nabet et al. [21]. The thesis' results are all concerned with the model by Nabet et al. [21], which considers only orientations and keeps the preferences constant.

1.1 Examples of synchronization studies in phase oscillator networks

The Kuramoto model is the simplest example of a class of models for coupled oscillators where each oscillator is reduced to a phase variable. In this section we will review three phase oscillator models that represent a population of oscillators such that each oscillator has a natural frequency.

Fireflies The model for synchronization of fireflies by Ermentrout [8] adds inertia to each oscillator phase. It simulates an experiment that required observing the change in the firing of a firefly when being exposed to flashing light. In this study a mechanism was proposed to explain how a firefly changes the timing of its firing in response to light flashes and the the Kuramoto model was modified accordingly by making frequency of oscillators adaptive. The following system represents a population of oscillators based on the light flash experiment

$$\frac{d\theta_j}{dt} = \omega_j,$$

$$\frac{d\omega_j}{dt} = \epsilon(\tilde{\omega}_j - \omega_j) + \sum_k P_{kj}(\theta_k) G_j(\omega_j, \theta_j).$$

The frequency ω_j is a function of time, giving each oscillator (θ_j, ω_j) inertia. The factor ϵ measures the preference of each oscillator for its intrinsic frequency $\tilde{\omega}_j$. The coupling function $P_{kj}(\theta_k)$ is the strength of the pulse of oscillator k, as observed by oscillator j (assumed to be of Gaussian shape by [8]). The function $G_j(\omega_j, \theta_j)$ is proportional to the *phase response curve* of oscillator j for ω_j, measuring the sensitivity of the oscillator to the stimuli. The model showed synchronization for coupling functions P_{kj} representing coupling of fireflys located on an irregular grid (one foot spaced apart) and able to see their neighbors within 3 feet range. The simulation results indicated that the oscillator representing the firefly adapted slowly to the stimuli (light flashes) by their neighbors.

Neurons The model by Tass [24] studies the firing of neurons. According to the study, the cause of tremor symptoms in Parkinson's disease is the synchronisation between the firing of neurons. To include the impact of the stimuli that encourages desynchronisation between neurons and tremor, the Kuramoto model was modified

to

$$\dot{\psi}_j = \Omega - \frac{K}{N}\sum_{k=1}^{N}\sin(\psi_j - \psi_k) + X_j(t)S_j(\psi_j) + F_j(t).$$

Here Ω is a uniform natural frequency of the oscillators, $S_j(\psi_j)$ are the external stimuli and $X_j(t)$ is a function that turns the stimuli on and off by switching between 0 and 1. The term $F_j(t)$ is a noise term. Tass [24] used this model to design phase resetting stimuli by choosing X_j in a way the destroys synchronization. Hence, these stimuli suppress tremor symptoms and could be applied as a strategy in deep brain stimulation treatments for Parkinson's disease.

Pedestrians A model by Strogatz et al. [23] considered the bridge as a weakly damped linear oscillator $X(t)$ that is forced by the sum of the force created by the humans gait of the pedestrians. Each human walking on the bridge is modelled with a differential equation of a phase oscillator Θ_i. The oscillator Θ_i has a random natural walking frequency Ω_i and is forced by the phase difference between the bridge vibration and the human gait, $\sin(\Psi - \Theta_i - \alpha)$. Here $X = A\sin\Psi$, and α is a phase lag parameter. The simulations showed that there is a threshold in the number of walkers. If the number of walkers is above this threshold then the bridge oscillates with an uncomfortably large amplitude. The synchronization effect was caused by the weak feedback between each pedestrian and the bridge. This makes this model very similar to Kuramoto models with globally coupled phase oscillators and sinusoidal coupling. The authors derived a formula for the *order parameter* r, a number between 0 and 1 that measures how synchronized the oscillators are ($r = 1$ means perfect synchronization). The authors state that the bridge designing process should not assume that pedestrian forcing is random, but that spontaneous synchronization can occur in general.

1.2 Decision making in animal group motion

Section 1.1 discussed variants of the Kuramoto model where all oscillators have a natural frequency. Here we discuss other papers in the literature on phase oscillator models that use the phase to model the orientation of particles or individuals.

For example, the model of a random magnet at zero temperature by Mirollo and Strogatz [17] has the following form:

$$\dot{\theta}_i = \sin(\alpha_i - \theta_i) + \frac{K}{N}\sum_{j=1}^{N}\sin(\theta_j - \theta_i) \quad \text{for } i = 1, \ldots, N. \tag{1.2}$$

In model (1.2) the angles α_i represent the background magnetic field, while the coupling models the preference for mutual alignment of the spins. Mirollo and Strogatz [17] considered the background field as randomly uniformly distributed on the unit circle. The question arises whether the spin orientations θ_i align or distribute (measured using the global order parameter r), depending on the coupling strength K. Mirollo and Strogatz [17] found that in the limit $N \to \infty$ there are two sharp transitions: at $K = 2$ a disordered system ($r = 0$) jumps to a highly ordered state (r close to 1). At $K_c < 2$ a highly ordered state collapses to zero order. For K between K_c and 2 ordered and disordered state are both stable. The setup of random preferences α_i is rather far from the animal decision problems studied by Couzin et al. [5], Nabet et al. [21]: in (1.2) the preferences α_i are typically all different and all preferences are equally strong. This is in contrast to the animal decision problem, where most individuals are assumed to be uninformed and only a few different preferences are present among subgroups.

One of the most recognized contributions to study decision making in animals group mathematically is a paper by Couzin et al. [5]. In this paper a discrete time model was proposed for decision making in groups of animals travelling or foraging in the plane. The model describes decision making based on social interactions in the group and is discrete in time. Each of the N animals has a position $c_i \in \mathbb{R}^2$, and at each step the model determines a desired orientation $d_i \in \mathbb{R}^2$. The desired orientation d_i of animal i is influenced by forces:

- turn away from other animals from which i has distance smaller than some α (this has highest priority),
- align with, and get attracted to individuals from which i has distance larger than α and smaller than ρ,
- prefer some direction g_i with a certain weight ω (this applies only to a subset of animals, the so-called *informed* group.

At each step, after calculation of d_i, the animal changes its orientation v_i toward this desired orientation d_i with some rate and random disturbance, and moves

with unit speed. First Couzin et al. [5] consider what happens when there is one informed group (N_1 animals that all have the same preferred orientation g_1) and all other animals are *naive* (have no preferred direction). For this case they measure the accuracy with which the entire group follows the preferred direction g_1. They find that the whole group can achieve good accuracy with a bounded number of informed individuals for increasing overall group size N. Couzin et al. [5] also check if the group splits. They find a trade-off for the preference weight ω. If ω is too large (the informed individuals care much about the preference compared to the social forces) the group is more likely to split. If ω is small then the accuracy of the whole group is low. The second case considered by Couzin et al. [5] is when the population consists of three groups. One of them is naive and the other two are associated with different preferred orientations based on prior knowledge. This case was considered only with parameters where the whole group does not split. The question was asked, if the group moves in the average direction of the informed groups or if the group makes a decision in favour of one informed group. The study found that for small differences in the two preferred orientations the group averages, while for large differences the group chooses one of the choices (more likely following the larger group). The angles where a decision occurs can be decreased by feedback between strength of preference ω and current orientation v_i for informed individuals.

The most important quantity of the model by Couzin et al. [5] is the orientation of animals and the group. The position of animals is only used to determine which other animals one individual chooses to adjust its orientation.

A natural idealization of the animals-in-the-plane model by Couzin et al. [5] is to ignore the position of each individual and make the dynamics dependent only on orientation. Leonard et al. [16] developed a mathematical model that is only based on the orientation angle θ_i for animal $i \leq N$. In addition it multiplies the coupling force by a time-dependent factor a_{ij}. The factor a_{ij} is dynamically determined. It increases (up to 1) when animal i and j have angles differing by less than $\pi/2$. It decreases (to 0) if their angles differ by more then $\pi/2$. Leonard et al. [16] also studies the case of three groups: two groups of identical size ($N_1 = N_2$) have preferred directions ($\bar{\theta}_1 = 0$ and $\bar{\theta}_2 \in [0, \pi]$), conflicting with each other. The third group has no preference. The model has a slow and a fast times scale. During the fast time scale all coupling factors a_{ij} settle to either 0 or 1, identically for each group. This means that the model has eight slow manifolds. Each manifold corresponds a connection configuration between groups. Stability conditions of these manifolds were stated

through finding critical values of $\bar{\theta}_2$ that correspond to the phase difference between the preferred direction of informed groups.

A simpler model than the model in Leonard et al. [16] was proposed by Nabet et al. [21]. The model has the following assumptions

- There is no dynamic adaptation of the coupling factors,
- they assume that all social forces are uniform (all-to-all coupling with strength K/N), and
- they consider the case of at most three subgroups: two informed groups, $\aleph_1$ and $\aleph_2 \subset \{1, \ldots, N\}$, with conflicting preferred directions $\bar{\theta}_1$ and $\bar{\theta}_2$, and one naive group, $\aleph_3$.

Each individual in the population is a particle moving in the plane at constant speed and the orientation of the particle takes any value from circle S_1. The two groups with preferred directions may model prior knowledge of migration route or food resource. The remaining group is attracted to the mean orientation of the migrating population. With these assumptions into account Nabet et al. [21] formulate the following system of differential equations governing the individuals' orientations θ_j:

$$\begin{aligned}
\dot{\theta}_j &= \sin\left(\bar{\theta}_1 - \theta_j\right) + \frac{K}{N}\sum_{\ell=1}^{N}\sin(\theta_\ell - \theta_j), \quad j \in \aleph_1, \\
\dot{\theta}_j &= \sin\left(\bar{\theta}_2 - \theta_j\right) + \frac{K}{N}\sum_{\ell=1}^{N}\sin(\theta_\ell - \theta_j), \quad j \in \aleph_2, \\
\dot{\theta}_j &= \frac{K}{N}\sum_{\ell=1}^{N}\sin(\theta_\ell - \theta_j), \quad j \in \aleph_3.
\end{aligned} \tag{1.3}$$

where $\bar{\theta}_k$ is the preferred direction associated with group $\aleph_k$ for $k = 1, 2$ (informed groups). The group denoted by $\aleph_3$ is naive group. We denote N_j the size of each group $\aleph_j$. Putting all three groups together gives the size $N = N_1 + N_2 + N_3$ of the entire population. Above N in the numerator we have the coupling strength K. This thesis will also study models of type (1.3) and generalizations, and we will call the terms $\sin(\bar{\theta}_k - \theta_j)$ for $k = 1, 2$ the *bias force*, and the term $\frac{K}{N}\sum_{\ell=1}^{N}\sin(\theta_\ell - \theta_j)$ the *coupling force*.

Nabet et al. [21] observed in simulations of (1.3) that the system has two time scales. On the fast time scale all individuals within each group synchronize. On the slow time scale the groups move relative to each other. They employed singular

perturbation theory to reduce the model. The small singular perturbation parameter is $\epsilon := 1/K$. For the reduction to be valid they need to make the assumptions that $K \gg N$ and that N_j are of the same order as N for $j = 1, 2$. Section 2.3.2 of this thesis proves that any equilibria must be unstable if members of the same group have different orientations θ_j. Together with the gradient structure of (1.3) (see Section 2.2) this implies that it is enough to study equilibria where all groups are synchronized, that is, $\theta_j = \Psi_k$ if $j \in \aleph_k$. This group-wise synchronized set is invariant in (1.3) even without time scale separation.

Nabet et al. [21] then proceed with a detailed bifurcation analysis of the case where all groups are synchronized (their slow dynamics). For the sake of simplicity they considered initially the case that the naive group is not present ($N_3 = 0$) and the other two groups have equal strength ($N_1 = N_2$), and studied the bifurcations of the reduced model,

$$\begin{aligned} \dot{\Psi}_1 &= \sin\left(\bar{\theta}_1 - \Psi_1\right) + \frac{K}{2}\sin(\Psi_2 - \Psi_1), \\ \dot{\Psi}_2 &= \sin\left(\bar{\theta}_2 - \Psi_2\right) + \frac{K}{2}\sin(\Psi_1 - \Psi_2), \end{aligned} \tag{1.4}$$

where Ψ_1 is the group with the preferred direction $\bar{\theta}_1$ and Ψ_2 is the group with the preferred direction $\bar{\theta}_2$. The preferred direction of one group, for example $\bar{\theta}_1$, can be set to zero without loss of generality, $\bar{\theta}_1 = 0$, such that the system has only two parameters, coupling strength $K \geq 0$, and difference $\bar{\theta}_2$ of the preferred orientations. As (1.3) is a gradient system, it is enough to study bifurcations of equilibria of (1.4).

Nabet et al. [21] found six equilibria of (1.4) divided into three sets (or types) of two. One may see this from adding the two equations in (1.3), which implies that either $\Psi_1 = \Psi_2 + \pi - \bar{\theta}_2$, or $\Psi_1 = \bar{\theta}_2 - \Psi_2$. The two equilibria satisfying the first condition, denoted by ψ_{S1}, ψ_{S2}, are always unstable, except when $K = 2$, $\bar{\theta}_2 = \pi/2$. In this special point they are equal and have double eigenvalue zero. The second condition implies that the mean of the two group orientations, $\frac{(\Psi_1+\Psi_2)}{2}$ is identical to the mean of the preferences (or facing in the opposite direction). Depending on K there is either one pair, called ψ_{sync1}, $\psi_{\text{antisync1}}$ of equilibria corresponding to this case, or, for K greater than some critical K_1, two pairs. The pair which exists only for $K > K_1$ is called ψ_{sync2}, $\psi_{\text{antisync2}}$ in the convention of Nabet et al. [21].

Of those up to 4 equilibria, ψ_{sync1} is always stable (and exists for all K). For $\bar{\theta}_2 \in [0, \pi]$ it corresponds to the configuration $0 \leq \Psi_1 \leq \bar{\theta}_2/2 \leq \Psi_2 \leq \bar{\theta}_2 \leq \pi$, where ψ_{s1}, ψ_{s2} are equal at $K = K_0$ and then both equilibria vanish when K is beyond K_0 in a reverse symmetry breaking bifurcation. Of the other equilibria only ψ_{sync2} is stable

in a parameter range (K_1, K_0), in which it coexists with the stable equilibrium ψ_{sync1} in this parameter region. The nature of ψ_{sync2} is most apparent for the symmetric case $\bar{\theta}_2 = \pi$ (both groups have diametrically opposite preferred orientation) and large K. In this case K_1 is the value of a pitchfork bifurcation for $\psi_{\text{sync1}} = (0, \pi)$, and ψ_{sync2} is the symmetric counterpart for ψ_{sync1}, $\psi_{\text{sync2}} = -\psi_{\text{sync1}}$, existing for $K > K_1$ ($K_0 = \infty$ for $\bar{\theta}_2 = \pi$).

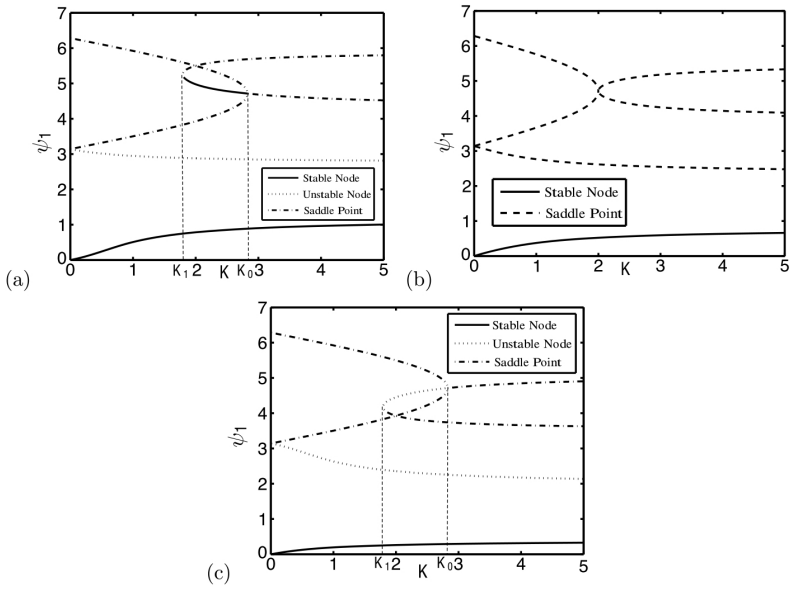

Fig. 1.1 (Reproduced from Nabet et al. [21] (copyright by Springer Science Business Media, LLC), permission requested) Bifurcation diagrams in cases (a) $\bar{\theta}_2 = \frac{3\pi}{4}$, (b) $\bar{\theta}_2 = \frac{\pi}{2}$, (c) $\bar{\theta}_2 = \frac{\pi}{4}$

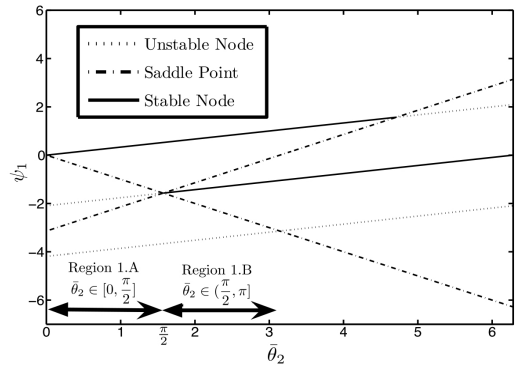

Fig. 1.2 (Reproduced from Nabet et al. [21] (copyright by Springer Science Business Media, LLC), permission requested) Bifurcations diagrams in $\bar{\theta}_2$ for fixed $K = 2$ showing bistability

In summary, Nabet et al. [21] find one stable equilibrium ψ_{sync1} which exists for all parameter values, and another stable equilibrium ψ_{sync2}, which coexists with ψ_{sync1}, in the region (see Lemmas 3.4 and 3.5 Nabet et al. [21])

$$K \in (K_1(\bar{\theta}_2), K_0(\bar{\theta}_2)) = \left(\left(\cos^{\frac{2}{3}} \left[\frac{\bar{\theta}_2}{2} \right] \sin^{\frac{2}{3}} \left[\frac{\bar{\theta}_2}{2} \right] \right)^{\frac{3}{2}}, \frac{2}{\sin \bar{\theta}_2} \right).$$

Nabet et al. [21] presented their bifurcation analysis of the case with two groups with conflicting information as a sequence of existence and stability lemmas, with bifurcations diagrams. Section 3.2 presents bifurcation diagrams (computed with coco [6, 7]) for the case of three groups (two with conflicting information, one uninformed). These diagrams will show that the structure is similar when a naive group is included.

The bifurcation analysis by Nabet et al. [21] proved that in the simple model (1.4) both informed groups will always by symmetric with respect to their preferred directions ($\Psi_1 + \Psi_2 = \bar{\theta}_1 + \bar{\theta}_2$) in stable equilibria. So, no group can "win over" the others for $N_1 = N_2$ by spontaneous symmetry breaking. This is a qualitative restriction making the model unable to reproduce the observations of the more complex model in Couzin et al. [5], where the simulation results showed that it is possible that one of the informed groups is dominant under some circumstances. Thus, Nabet et al. [21] modified (1.4) enabling the population to choose one of the preferred directions. The modification multiplied the bias force by the following Gaussian shaped gain that is called forgetting feedback factor in Nabet et al. [21]

$$\exp\left(-\frac{\sin(\bar{\theta}_k - \Psi_k)}{\alpha} \right) \quad \text{for} \quad k = 1, 2 \tag{1.5}$$

where α is a positive constant that controls the standard deviation in the population represented by the Gaussian distribution. The results of the modified model were illustrated through a bifurcation diagram for an example fixed $K = 2.5$ and $\alpha = 0.2$, varying the difference $\bar{\theta}_1 - \bar{\theta}_2$ between preferences. The bifurcation diagram showed that beyond a critical value $\bar{\theta_2}^*$ the equilibrium where both groups are symmetric about the averaged direction loses its stability and new branches appear. Each of the new branches corresponds to the population heading in the mean towards either of the preferred directions. This corresponds to the desired decision making effect. For groups of different size ($N_1 \neq N_2$) the results in [21] showed that the mean of

the group orientations will be a weighted average of the preferred directions. It will give more weight to the larger group.

Nabet [19] also demonstrated the robustness of the results for (1.3) to random heterogeneity introduced within each group. The probability of settling near ψ_{sync1} or ψ_{sync2} estimated the basin of attraction for the respective equilibria. Increasing the coupling strength K reduced the visible effect of the heterogeneity.

Chapter 2

Longtime behaviour of oscillator network

2.1 Introduction

In this chapter we focus on the properties of the phase oscillator model (1.3) for orientation dynamics. We first observe the well-known fact (see Nabet [19] and Brown et al. [2]) that the system has a gradient structure in Section 2.2, repeating the short proof. Section 2.3 contains new results, which show that in general we will have for almost all initial conditions asymptotic alignment within groups (that is, between individuals with identical bias forces). The arguments in Section 2.3 rely on the gradient structure to rule out non-trivial asymptotic dynamics as they only consider equilibria and their stability. They also use that equilibria have symmetric Jacobian matrices in gradient systems. Section 2.3.3 improves the singular perturbation analysis of Nabet [19] by showing that for small bias forces we have a one-dimensional slow manifold. Section 2.4 shows that the result on almost sure alignment depends on the harmonic coupling. An arbitrarily small perturbation in the coupling can lead to group splitting. Throughout this chapter we will work with the following more compact and more general form of (1.3)

$$\dot{\theta}_j = \delta a_j \sin(\bar{\theta}_j - \theta_j) + \frac{1}{N}\sum_{l=1}^{N} \sin(\theta_l - \theta_j) \quad \text{for} j = 1...N \tag{2.1}$$

where a_j are arbitrary factors that indicate the strength of preference of individual j for angle θ_j (which is also arbitrary). Comparing (2.1) to the three-group model (1.3) studied by Nabet et al. [21] we note that time has been rescaled by K and that the

parameter δ is equal to $\frac{1}{K}$ in (1.3). This is a slight generalization of system used by Mirollo and Strogatz [17] as coupled spin model, when they considered transitions with respect to δ of the system in the limit $N \to \infty$. (Mirollo and Strogatz [17] considered a uniform $a_j = 1$.) The result of an illustrative numerical simulation of system (2.1) is shown in figure 2.1. For the simulation we fixed $\bar{\theta}_j = 0$, $a_j = 1$ for $j = 1, \ldots, 5$, $\bar{\theta}_j = 2$, $a_j = 1$ for $j = 6, \ldots, 10$, $a_j = 0$ for $j = 11, \ldots, 15$ such that the individuals for three groups (overall $N = 15$, $\delta = 1$). This figure shows that individuals belonging to the same group start (that is, with the same a_j and θ_j) converge to each other after a very short time even if they start with different initial conditions. We call this behaviour (in-group) synchronisation. We note that the initial conditions were selected randomly. These observations suggest that

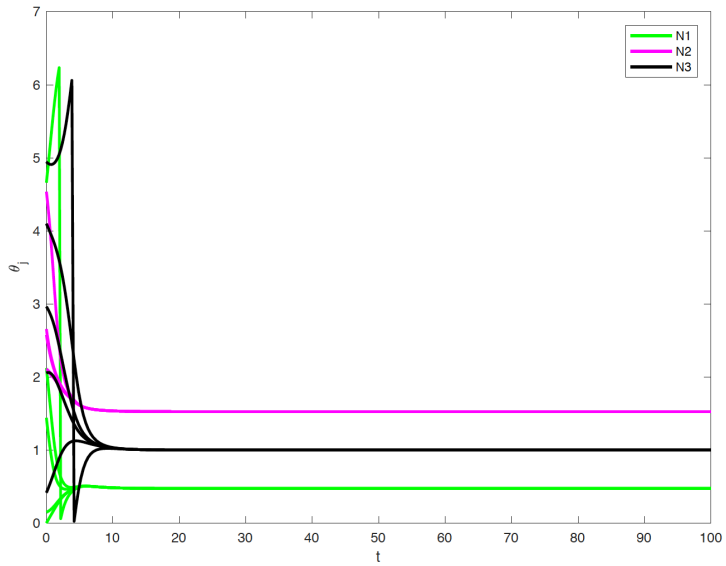

Fig. 2.1 Time profile for multi-agent system. N_1(individuals following $\bar{\theta}_1$) $= 5$, N_2(individuals following $\bar{\theta}_2$) $= 5$, N_3(Naive individuals) $= 5$, $\bar{\theta}_1 = 0, \bar{\theta}_2 = 2$, $\delta = 1$

(a) the stable long-time behaviour of (2.1) is convergence to an equilibrium, and

(b) individuals with the same preference converge to the same asymptotic angle (that is, if $a_j = a_k$ and $\bar{\theta}_j = \bar{\theta}_k$, then $\theta_j(t) - \theta_k(t) \to 0$ for $t \to \infty$).

However, the computational illustration in Figure 2.1 was only performed for our particular choice of parameters. The following sections prove the claims above rigorously. During the proofs we employ the concept of complex order parameter

which was introduced in [14] to study stability of all different kinds of equilibria. The methodology in this chapter works even for high dimensional systems. In the following sections we verify that the the oscillator model is gradient, study the stability of equilibria for different choices of preferred direction strength and the last section will be dedicated for studying the impact of changing the coupling function.

2.2 Existence of a potential

The right-hand side of system of coupled oscillators (2.1) is coupled with a purely sinusoidal coupling function which is an odd function. According to Brown et al. [2] this system has gradient structure with a potential function $\mathcal{V}$ for all parameters. Systems of this type are said to have *gradient structure*, defined as follows:

Definition 1. *[10] A differential equation $\dot{\boldsymbol{\theta}} = \boldsymbol{F}(\boldsymbol{\theta})$ with $\boldsymbol{\theta}, \boldsymbol{F}(\boldsymbol{\theta}) \in \mathbb{R}^N$ is said to have gradient structure if there exists a function $\mathcal{V} : \mathbb{R}^N \to \mathbb{R}$ such that $\boldsymbol{F}(\boldsymbol{\theta}) = -\operatorname{grad} \mathcal{V}(\boldsymbol{\theta})$ for all $\boldsymbol{\theta} \in \mathbb{R}^N$. where $\mathcal{V} : \mathbb{R}^N \to \mathbb{R}^1$ is continuously differentiable twice, and*

$$\operatorname{grad} \mathcal{V} = \left(\frac{\partial \mathcal{V}}{\partial \theta_1}, ..., \frac{\partial \mathcal{V}}{\partial \theta_N} \right).$$

Lemma 1. *System* (2.1) *has the potential*

$$\mathcal{V}(\theta_1, ..., \theta_2) = -\sum_{j=1}^{N} \left[\delta a_j \cos\left(\bar{\theta}_j - \theta_j\right) + \frac{1}{2N} \sum_{\ell=1}^{N} \cos(\theta_\ell - \theta_j) \right] \tag{2.2}$$

Proof. Consider differentiating $\mathcal{V}$ with respect to θ_j for $j = 1, .., N$

$$\frac{\partial \mathcal{V}}{\partial \theta_j} = \delta a_j \sin(\bar{\theta}_j - \theta_j) + \frac{1}{N} \sum_{\ell=1}^{N} \sin(\theta_\ell - \theta_j) \quad \text{for} j = 1...N \tag{2.3}$$

Since the right hand side of (2.3) is equal to the right hand side of (2.1), the function $\mathcal{V}$ is a potential function for (2.1). □

Now that we found the potential function, we can apply theorems for gradient systems to constrain how orbits behave.

Proposition 1. *[10] The function $\mathcal{V}$ is strictly decreasing along non constant solutions of the system*
$\dot{\boldsymbol{\theta}} = -$ grad $\mathcal{V}(\boldsymbol{\theta})$. Moreover, $\dot{\mathcal{V}}(\boldsymbol{\theta}) = 0$ if and only if $\boldsymbol{\theta}$ is an equilibrium point

Proof. In order to check how orbits behave, we differentiate $\mathcal{V}$ with respect to time. Following from chain rule

$$\dot{\mathcal{V}}(\boldsymbol{\theta}) = \frac{d\mathcal{V}}{d\boldsymbol{\theta}} \cdot \frac{d\boldsymbol{\theta}}{dt} \tag{2.4}$$

Thus, we have

$$\dot{\mathcal{V}}(\boldsymbol{\theta}) = \operatorname{grad} \mathcal{V}(\boldsymbol{\theta}) \cdot (-\operatorname{grad} \mathcal{V}(\boldsymbol{\theta}))$$

The right hand side is equal to

$$-|\text{grad}\mathcal{V}(\boldsymbol{\theta})|^2 \leq 0$$

The expression is always decreasing when $\operatorname{grad} \mathcal{V} \neq 0$ and equal to zero at critical points of $\mathcal{V}$, which are the equilibria of the gradient system. □

Given that the function $\mathcal{V}$ is monotone decreasing, there are no periodic orbits or heteroclinic cycles. Moreover, the Jacobian of a gradient system has the following form

$$J = -\begin{bmatrix} \frac{\partial^2 \mathcal{V}}{\partial \theta_1^2} & \frac{\partial^2 \mathcal{V}}{\partial \theta_1 \partial \theta_2} & \cdots & \frac{\partial^2 \mathcal{V}}{\partial \theta_1 \partial \theta_N} \\ \frac{\partial^2 \mathcal{V}}{\partial \theta_2 \partial \theta_1} & \frac{\partial^2 \mathcal{V}}{\partial \theta_2^2} & \cdots & \frac{\partial^2 \mathcal{V}}{\partial \theta_2 \partial \theta_N} \\ \vdots & \vdots & \ddots & \vdots \\ \frac{\partial^2 \mathcal{V}}{\partial \theta_N \theta_1} & \frac{\partial^2 \mathcal{V}}{\partial \theta_N \partial \theta_2} & \cdots & \frac{\partial^2 \mathcal{V}}{\partial \theta_N^2} \end{bmatrix}$$

This Jacobian of $\operatorname{grad}(\mathcal{V})$ is commonly known as the Hessian matrix of $\mathcal{V}$, which is symmetric. For further reading about hessian matrix see chapter 3 in [25]. Thus, all eigenvalues of J are real and there are no closed orbits. We also recall that, if a symmetric matrix has positive diagonal elements, one of its eigenvalues must have positive real part. This follows from the fact that the sum of diagonal elements of a symmetric matrix is equal to the sum of its eigenvalues. For further information see Chan and Li [3]. We will use this below to conclude that equilibria are unstable if two angles are different despite identical bias strength and angle.

2.3 Synchronicity and Stability of Equilibria

The system (2.1) has the following Jacobian B

$$b_{ij} = \begin{cases} -\delta a_j \cos(\bar{\theta}_j - \theta_j) + \frac{1}{N} - \frac{1}{N} \sum_{\ell=1}^{N} \cos(\theta_\ell - \theta_j) & \text{if i} = j \\ \frac{1}{N} \cos(\theta_i - \theta_j) & \text{if i} \neq j \end{cases} \tag{2.5}$$

Due to the gradient structure, the Jacobian is symmetric. The sum of eigenvalues is equal to the trace [9]. Recall that a_j was the strength of preference. We consider three cases. For the first case we set $a_j = 0$ for all j. For the second case we set a_j arbitrary such that we may set $\delta = 1$ without loss of generality. The third case requires setting $\delta \approx 0$

2.3.1 No bias force: $a_j = 0$ for all j

Setting $a_j = 0$ gives the following system

$$\dot{\theta}_j = \frac{1}{N} \sum_{\ell=1}^{N} \sin(\theta_\ell - \theta_j) \quad \text{for} \quad j = 1...N. \tag{2.6}$$

We observe that (2.6) has rotational symmetry: if $(\theta_1(t), \ldots, \theta_N(t))$ is a solution of (2.6), then $(\theta_1(t) + \omega, \ldots, \theta_N(t) + \omega)$ is also a solution for every $\omega \in [0, 2\pi)$. This section will show that for (2.6) only the fully synchronized equilibria ($\theta_1 = \ldots = \theta_N$) are stable (up to a rotation by arbitrary ω), while all other equilibria are unstable. This result can also be found in Brown et al. [2]. The Jacobian B of (2.6) is

$$B_{ij} = \begin{cases} \frac{1}{N} - \frac{1}{N} \sum_{\ell=1}^{N} \cos(\theta_\ell - \theta_j) & \text{if i=}j \\ \frac{1}{N} \cos(\theta_i - \theta_j) & \text{if i} \neq j \end{cases} \tag{2.7}$$

Since $\cos x$ is an even function, the Jacobian B is symmetric. Each diagonal element is equal to $\frac{1}{N} - \frac{1}{N} \sum_{\ell=1}^{N} \cos(\theta_l - \theta_j)$, where the term $\frac{1}{N}$ compensates for $\cos(\theta_j - \theta_j)$. Summing all diagonal elements gives

$$\operatorname{tr} B = 1 - \sum_{j=1}^{N} \left(\frac{1}{N} \sum_{\ell=1}^{N} \cos(\theta_\ell - \theta_j) \right) = 1 - N \left(\frac{1}{N} \sum_{\ell=1}^{N} \cos(\theta_\ell - \theta_j) \right) \tag{2.8}$$

We note that the the term $\frac{1}{N} \sum_{\ell=1}^{N} \cos(\theta_l - \theta_j)$ is equal to the modulus of complex order parameter, defined as

$$r = \frac{1}{N} \sum_{\ell=1}^{N} \exp(\mathrm{i}\theta_\ell). \tag{2.9}$$

The complex order r is the average of all positions, when considering the positions as points on the unit circle. Inserting r into (2.8) gives

$$\operatorname{tr} B = 1 - N|r|^2 \tag{2.10}$$

At fully synchronised equilibria r will be equal to 1, whereas at desynchronised equilibria (when the orientations of all individuals are evenly spread on unit circle) r will be equal to 0. To track the change of the averaged angle we define the kth order parameter for integers k (including 0 and negative):

$$r_k = \frac{1}{N}\sum_{\ell=1}^{N} \exp(\mathrm{i}k\theta_\ell). \tag{2.11}$$

Thus, $r_0 = 1$ and $r_{-k} = \bar{r}_k$ for all $k \in \mathbb{Z}$. Taking the time derivative of the kth order parameter gives

$$\dot{r}_k = \frac{1}{N}\sum_{\ell=1}^{N} \exp(\mathrm{i}k\theta_\ell) \cdot \mathrm{i}k\dot{\theta}_l. \tag{2.12}$$

Substituting the right hand side of (2.6) into (2.12) gives

$$\dot{r}_k = \frac{1}{N}\sum_{\ell=1}^{N} \exp(\mathrm{i}k\theta_\ell) \cdot \frac{\mathrm{i}k}{N}\sum_{\ell=1}^{N} \sin(\theta_\ell - \theta_j). \tag{2.13}$$

Using the definition $\sin x = (\exp(\mathrm{i}x) - \exp(-\mathrm{i}x))/(2\mathrm{i})$
and expanding the product in (2.13) gives

$$\dot{r}_k = \frac{k}{2N}\sum_{\ell=1}^{N}\frac{1}{N}\sum_{j=1}^{N} \exp[\mathrm{i}\theta_j + \mathrm{i}(k-1)\theta_\ell] - \exp[\mathrm{i}(k+1)\theta_\ell - \mathrm{i}\theta_j] \tag{2.14}$$

Applying the definition of the order parameter to (2.14) gives a differential equation for each order parameter r_k

$$\dot{r}_k = \frac{k}{2}[r_1 r_{k-1} - r_{k+1} r_{-1}] \tag{2.15}$$

Given that complex order parameter is time dependent, at equilibria these order parameters satisfy $\dot{r}_k = 0$, $k \in \mathbb{Z}$. For $k = 1$ this implies

$$\dot{r}_1 = \frac{1}{2}[r_1 - r_2 r_{-1}] \tag{2.16}$$

Since r_{-1} is the conjugate of r_1 and r_2 has modulus less or equal than unity, we have two cases that satisfy $\dot{r}_1$ is equal to zero. The first case is that r_1 is equal to 0, the second case is that $|r_1| > 0$ such that $|r_2|$ must be equal to 1. If $r_1 = 0$, then (by (2.10)) $\operatorname{tr} B > 0$ such that the equilibrium must be unstable. If $|r_2| = 1$ in the equilibrium $(\theta_1, \ldots, \theta_N)$, this implies that the doubles of all angles are equal to each other. If r_2 has the form $\exp(2\mathrm{i}\omega)$ for some $\omega \in [0, 2\pi)$, we may consider the equilibrium shifted by ω, $(\theta_1 - \omega, \ldots, \theta_N - \omega)$ (because of rotational symmetry), which has the same stability properties as $(\theta_1, \ldots, \theta_N)$ instead, but the equilibrium that is shifted by ω has $r_2 = 1$. Thus, we may, without loss of generality, assume that $r_2 = 1$ such that θ_j are equal to multiples of π for all j. For this reason we set $\theta_j = 0$ for $j \leq N_1$ and for $j > N_1$ we set $\theta_j = \pi$. The Jacobian B in this case contains the following elements ($N_2 = N - N_1$)

$$B_{ij} = \begin{cases} \frac{N_2 - N_1 + 1}{N} & \text{if } i{=}j \text{ and i} \leq N_1 \\ \frac{N_1 - N_2 + 1}{N} & \text{if } i = j \text{ and i} > N_1 \\ \frac{1}{N} & \text{if } i \neq j \text{ and both } i, j \leq N_1 \text{ or both } i, j > N_1 \\ -\frac{1}{N} & \text{if } i \neq j \text{ and } i \leq N_1 \text{ and } j > N_1, \text{ or } i > N_1 \text{ and } j \leq N_1. \end{cases} \tag{2.17}$$

We will show that B has an eigenvalue 1 with an eigenvector v of the form

$$v_i = \begin{cases} a & \text{if } i \leq N_1 \\ b & \text{if } i > N_1 \end{cases} \tag{2.18}$$

Then Bv has the entries

$$(Bv)_i = \begin{cases} \frac{1}{N}\big(- N_2 b + N_2 a\big) & \text{if } i \leq N_1 \\ \frac{1}{N}\big(- N_1 a + N_1 b\big) & \text{if } i > N_1 \end{cases} \tag{2.19}$$

The product Bv is equal to v if and only if:

- $\frac{1}{N}\big(- N_2 b + N_2 a\big) = a$. This condition holds if and only if $-N_2 b = N_1 a$
- $\frac{1}{N}\big(- N_1 a + N_1 b\big) = b$. This condition holds if and only if $-N_2 b = N_1 a$

By letting $a = N_2 \quad \text{and} \quad b = -N_1$, we get an eigenvector of the Jacobian B associated with the eigenvalue 1. Thus, the equilibria such that $r_2 = 1$ are unstable. This leaves equilibria with $r_1 = 1$ as the only potentially stable equilibria.

For $r_1 = 1$ all θ_j are equal such that the Jaocbian B has the entries $-(N-1)/N$ on the diagonal and $1/N$ off the main diagonal. Its eigenvalues are 0 (single) and -1 (multiplicity $N-1$). Consequently, all fully synchronized equilibria are stable apart from the invariance with respect to rotation around the circle. Generally, if $\boldsymbol{\theta}(t)$ is a solution of (2.6) then $\boldsymbol{\theta}(t) + \phi$ is also a solution for any $\phi \in \mathbb{R}$, where the addition of ϕ to $\boldsymbol{\theta}$ is component-wise. Correspondingly, the eigenvector for the eigenvalue 0 equals $(1, \ldots, 1)^T \in \mathbb{R}^N$.

2.3.2 General case: arbitrary a_j

We now generalize the above argument to the case where individuals have arbitrary bias strength a_j and arbitrary preference angles $\bar{\theta}_j$. Consider the following system of differential equations

$$\dot{\theta}_j = a_j \sin(\bar{\theta}_j - \theta_j) + \frac{1}{N} \sum_{\ell=1}^{N} \sin(\theta_\ell - \theta_j) \quad \text{for} j = 1...N \tag{2.20}$$

with arbitrary a_j and $\bar{\theta}_j$, where we dropped the common factor δ for the bias forces without loss of generality.

Lemma 2 (Desynchronised equilibria are unstable)**.** *Let $G = \{1, \ldots, N_g\}$ be a group of indices such that the preference strengths a_j and angles $\bar{\theta}_j$ are all identical for $j \leq N_g$ ($a_j = a_g$, $\bar{\theta}_j = \bar{\theta}_g$ for $j \leq N_g$). Let $\theta \in \mathbb{R}^N$ be an equilibrium of* (2.20) *for which $\theta_m \neq \theta_n$ for some $m, n \in N_g$. Then θ is linearly unstable.*

Proof. Given that the population consists of a group G that is distinguished from the rest of the population by the preferred direction and there are two individuals m, n within the group who are not synchronised with the rest of group members and distinct from each other at equilibrium, we introduce the local order parameter for group G in (2.21) and the mean external influence on group G in (2.22)

$$r_{g,k} = \frac{1}{N_g} \sum_{j=1}^{N_g} \exp(\mathrm{i}k\theta_j) \tag{2.21}$$

$$s_{g,k} = \frac{N}{N_g} a_g \exp(\mathrm{i}k\bar{\theta}_g) + \frac{1}{N_g} \sum_{j=N_g+1}^{N} \exp(\mathrm{i}k\theta_j) \tag{2.22}$$

Consider the time derivative of $\exp(\mathrm{i}k\theta_j)$

$$\mathrm{i}\exp(\mathrm{i}\theta_j)\cdot\dot{\theta}_j = \frac{a_j}{2}\left(\exp\mathrm{i}(\bar{\theta}_j) - \exp\left[-\mathrm{i}(\bar{\theta}_j - 2\theta_j)\right]\right) + \frac{1}{2N}\sum_{\ell=1}^{N}\exp(\mathrm{i}\theta_\ell) - \exp\left[\mathrm{i}(2\theta_j - \theta_\ell)\right] \tag{2.23}$$

The right hand side in (2.23) is a result of using the definition of $\dot{\theta}_j$ from (2.20). Rearranging all terms and factoring all terms multiplied by $\exp(2\mathrm{i}\theta_j)$ gives

$$\mathrm{i}\exp(\mathrm{i}\theta_j)\cdot\dot{\theta}_j = \frac{a_j}{2}\exp(\mathrm{i}\bar{\theta}_j) + \frac{1}{2N}\sum_{\ell=1}^{N}\exp(\mathrm{i}\theta_\ell) - \left[\frac{a_j}{2}\exp(-\mathrm{i}\bar{\theta}_j) + \frac{1}{2N}\sum_{\ell=1}^{N}\exp(-\mathrm{i}\theta_\ell)\right]\cdot\exp(2\mathrm{i}\theta_j) \tag{2.24}$$

Splitting up the sum $\frac{1}{2N}\sum_{\ell=1}^{N}\exp(\mathrm{i}\theta_\ell) = \frac{1}{2N}\left(\sum_{\ell=1}^{N_g}\exp(\mathrm{i}\theta_\ell) + \sum_{\ell=N_g+1}^{N}\exp(\mathrm{i}\theta_\ell)\right)$ and inserting $a_j = a_g$ and $\bar{\theta}_j = \bar{\theta}_g$ for all $j \in G$ gives

$$\mathrm{i}\exp(\mathrm{i}\theta_j)\cdot\dot{\theta}_j = \frac{N_g}{2N}\left[s_{g,1} + r_{g,1} - (s_{g,-1} + r_{g,-1})\exp(2\mathrm{i}\theta_j)\right] \tag{2.25}$$

Taking the mean over all $j \leq N_g$ of these equations, we obtain

$$\dot{r}_{g,1} = \frac{N_g}{2N}\left[s_{g,1} + r_{g,1} - r_{g,2}(s_{g,-1} + r_{g,-1})\right] = \frac{N_g}{2N}\left[s_{g,1} + r_{g,1} - r_{g,2}(\bar{s}_{g,1} + \bar{r}_{g,1})\right] \tag{2.26}$$

(note that $r_{g,-k}$ equals the complex conjugate $\bar{r}_{g,k}$ for all k and the same holds for $s_{g,k}$). Thus, if θ is an equilibrium, then $|r_{g,2}| = 1$ or $s_{g,1} = -r_{g,1}$(in case $|r_{g,2}| < 1$). Let us consider the diagonal elements for $j \leq N_g$ in the Jacobian B of (2.20) evaluated at the equilibrium:

$$\begin{aligned} b_{jj} &= -a_g\cos(\bar{\theta}_g - \theta_j) - \frac{1}{N}\sum_{\ell=1}^{N}\cos(\theta_\ell - \theta_j) + \frac{1}{N} \\ b_{jj} &= \frac{1}{N} - a_g\cos(\bar{\theta}_g - \theta_j) - \frac{1}{N}\sum_{\ell=1}^{N_g}\cos(\theta_\ell - \theta_j) - \frac{1}{N}\sum_{\ell=N_g+1}^{N}\cos(\theta_\ell - \theta_j) \end{aligned} \tag{2.27}$$

The term $\frac{1}{N}$ compensates for the term $\cos(\theta_j - \theta_j) = 1$ inside the sum. Writing the function $\cos x$ as $\frac{\exp(\mathrm{i}x)+\exp(-\mathrm{i}x)}{2}$, gives

$$\begin{aligned} b_{jj} =& \frac{1}{N} - \frac{a_g}{2}\big(\exp[\mathrm{i}(\bar{\theta}_g - \theta_j)] + \exp[\mathrm{i}(-\bar{\theta}_g + \theta_j)]\big) \\ &- \frac{1}{2N}\sum_{\ell=1}^{N_g}\big(\exp[\mathrm{i}(\theta_\ell - \theta_j)] + \exp[\mathrm{i}(-\theta_\ell + \theta_j)]\big) \\ &- \frac{1}{2N}\sum_{\ell=N_g+1}^{N}\big(\exp[\mathrm{i}(\theta_\ell - \theta_j)] + \exp[\mathrm{i}(-\theta_\ell + \theta_j)]\big) \end{aligned} \tag{2.28}$$

Factoring out the terms $\exp(\pm\mathrm{i}\theta_j)N_g/(2N)$ gives

$$\begin{aligned} b_{jj} = \frac{1}{N} &- \frac{N_g}{2N}\left[a_g 2N\exp(\mathrm{i}\theta_g) + \frac{1}{N_g}\sum_{\ell=N_g+1}^{N}\exp(\mathrm{i}\theta_\ell) + \frac{1}{N_g}\sum_{\ell=1}^{N_g}\exp(\mathrm{i}\theta_\ell)\right]\exp(-\mathrm{i}\theta_j) \\ &- \frac{N_g}{2N}\left[a_g 2N\exp(-\mathrm{i}\theta_g) + \frac{1}{N_g}\sum_{\ell=N_g+1}^{N}\exp(-\mathrm{i}\theta_\ell)\frac{1}{N_g} + \sum_{\ell=1}^{N_g}\exp(-\mathrm{i}\theta_\ell)\right]\exp(\mathrm{i}\theta_j) \end{aligned} \tag{2.29}$$

Following from the definitions of (2.21) and (2.22) for $r_{g,k}$ and $s_{g,k}$ we have

$$b_{jj} = \frac{1}{N} - \frac{N_g}{2N}(s_{g,1} + r_{g,1})\exp(-\mathrm{i}\theta_j) - \frac{N_g}{2N}(s_{g,-1} + r_{g,-1})\exp(\mathrm{i}\theta_j) \tag{2.30}$$

Consequently, for every equilibrium θ with $r_{g,1} + s_{g,1} = 0$ the diagonal elements of B such on rows $j \leq N_g$ are equal to $\frac{1}{N}$. Since B is symmetric, this implies that B has positive eigenvalues. Hence, we only need to investigate equilibria θ with $|r_{g,2}| = 1$ for (in)stability. We can assume without loss of generality that $r_{g,2} = 1$. This implies that $\theta_j = 0$ or $\theta_j = \pi$ for $j \leq N_g$. Let us assume that for some pair $m, n \leq N_1$ we have $\theta_m = 0$ and $\theta_n = \pi$. This assumption implies $\exp(\mathrm{i}\theta_m) = \exp(-\mathrm{i}\theta_m) = 1$ and $\exp(\mathrm{i}\theta_n) = \exp(-\mathrm{i}\theta_n) = -1$. Thus,

$$b_{mm} + b_{nn} = \frac{2}{N} \tag{2.31}$$

Hence, one of the diagonal elements of B, b_{mm} or b_{nn}, must be positive eigenvalues such that B must have positive eigenvalues. Consequently, the Jacobian B in an equilibrium has positive unless all θ_j are equal for $j \leq N_g$. □

Now that we proved that synchronised equilibria are the only stable equilibria for the general case and we already know that the system has a gradient structure (such that the $\omega-$limit set consists only of equilibria), we conclude:

Theorem 1 (Almost sure synchronisation)**.** *In* (2.20)*, for all initial conditions, except those in the stable manifolds of unstable equilibria,all oscillators within a group converge to the same limit. In particular, if* $a_j = a_i$ *and* $\bar{\theta}_j = \bar{\theta}_i$ *for some indices* i *and* j *then* $\theta_j(t) - \theta_i(t) \to 0$ *for* $t \to \infty$ *for almost all initial conditions* $\boldsymbol{\theta}(0)$ *of* (2.20)*.*

2.3.3 Special Case: Slow-fast system for $\delta \approx 0$

The previous section provides a general argument why it is sufficient to study the dynamics of N orientations θ_i on the subspace of S^N (the N-dimensional torus), where angles θ_i for individuals with the same preference (strength a_i and angle $\bar{\theta}_i$) are identical. Nabet et al. [21] gave a different argument, based on a slow-fast analysis in the limit of strong coupling K between oscillators. They considered the case of three groups, where two groups have different preference angles $\bar{\theta}_1$ and $\bar{\theta}_2$ but equal strength, and one group has no preference. They derive (3.1), which we will study in Section 3, as a reduced system on a three-dimensional slow manifold in the limit of large coupling coefficient K. However, a large coupling coefficient K is equivalent to a small preference factor δ and $K = 1$ in (2.1),

$$\dot{\theta}_i = \delta a_i \sin(\bar{\theta}_i - \theta_i) + \frac{1}{N}\sum_{k=1}^{N} \sin(\theta_k - \theta_i) \quad \text{for } i = 1\ldots, N. \tag{2.32}$$

However, our analysis in Section 2.3.1 showed that the manifold of stable equilibria for $\delta = 0$ is one-dimensional:

$$\mathcal{C}_0 = \{\theta \in S^N : \theta_1 = \ldots = \theta_N\}.$$

Consequently, we expect that the slow manifold $\mathcal{C}_\delta$ for (2.32) and small δ (same as large K) should also be one-dimensional, independent of the individual preference strengths a_j (as long as $\sum a_j^2 \approx 1$ in the scaling of (2.32)) and angles $\bar{\theta}_j$. This section derives the zero-order approximation of the flow on this one-dimensional slow manifold.

First we observe that (2.32) is not in a form where the slow and the fast subsystem are explicitly visible. However, this explicit slow-fast form can be obtained by a linear coordinate transformation. The Jacobian B of (2.32) in any point θ of the

manifold $\mathcal{C}_0$ for $\delta = 0$ is

$$B_{ij} = \begin{cases} \frac{1}{N} - \frac{1}{N}\sum_{\ell=1}^{N}\cos(\theta_l - \theta_j) = \frac{-(N-1)}{N} & \text{if i=}j \\ \frac{1}{N}\cos(\theta_i - \theta_j) = \frac{1}{N} & \text{if i} \neq j \end{cases} = -I + \frac{1}{N}\mathbb{1}_N, \tag{2.33}$$

where I is the $N \times N$ identity matrix and $\mathbb{1}$ is the $N \times N$ matrix with all entries equal to 1. Considering that the above matrix is symmetric we can find an orthogonal spectral decomposition. In the case of B the eigenvalue -1 has geometric multiplicity $N-1$ and the eigenvalue 0 has multiplicity 1. For further reading about spectral decomposition see chapter 7 in Lay [15]. Thus, B can be decomposed as

$$B = -QQ^T \tag{2.34}$$

where $Q \in \mathbb{R}^{N\times(N-1)}$ is orthogonal and of the form

$$Q_{i,m} = \begin{cases} \frac{1}{\sqrt{m+m^2}} & \text{if } i < m+1 \\ -\frac{m}{\sqrt{m+m^2}} & \text{if } i = m+1 \\ 0 & \text{if } i > m+1 \end{cases} \tag{2.35}$$

The unit eigenvector associated with the eigenvalue $\lambda = 0$ is

$$V = \begin{bmatrix} \frac{1}{\sqrt{N}} \\ \vdots \\ \frac{1}{\sqrt{N}} \end{bmatrix} \in \mathbb{R}^{N\times 1}. \tag{2.36}$$

This vector V is the unit tangent vector to the manifold $\mathcal{C}_{\prime}$. We define

$$x = V^T\theta \in \mathbb{R}, \qquad\qquad y = Q^T\theta \in \mathbb{R}^{N-1}.$$

Then, $\theta = Vx + Qy$. We split the right hand side of the full system in (2.32) into two contributions using the functions

$$F_1 : \theta \in \mathbb{R}^N \mapsto \left(a_j \sin\left(\bar{\theta}_j - \theta_j\right)\right)_{j=1}^{N} \in \mathbb{R}^N$$
$$F_2 : \theta \in \mathbb{R}^N \mapsto \left(\frac{1}{N}\sum_{\ell=1}^{N}\sin(\theta_\ell - \theta_j)\right)_{j=1}^{N} \in \mathbb{R}^N,$$

dropping the arguments a and $\bar{\theta}$ from F_1. We note that $\partial F_2(\theta)V = 0$ for all θ. In this notation, (2.32) reads

$$\dot{\theta} = \delta F_1(\theta) + F_2(\theta). \tag{2.37}$$

Decomposing this equation by multiplying it with V^T and Q^T, and substituting $\theta = Vx + Qy$ on the right-hand side, we obtain the system

$$\dot{x} = \delta V^T F_1(Vx + Qy) + V^T F_2(Qy), \tag{2.38}$$
$$\dot{y} = \delta Q^T F_1(Vx + Qy) + Q^T F_2(Qy). \tag{2.39}$$

We have no dependence of F_2 on Vx since $\partial F_2(\theta)V = 0$ for all θ. For $\delta = 0$ equation has the stable equilibrium $y = 0$ for all x. Thus, y is the fast variable, and the manifold $\mathcal{C}_0$ can be written as $\{(x, y) \in \mathbb{R} \times \mathbb{R}^{N-1} : y = 0\}$ in (x, y) coordinates. For small δ this manifold will persist as a manifold $\mathcal{C}_\delta$. The perturbed manifold can be written as a graph $y(x, \delta)$, which we can expand in δ: $y(x, \delta) = \delta y_1(x) + O(\delta^2)$. We can obtain the first expansion coefficient $y_1(x)$ from (2.39) by inserting the expansion and comparing coefficients of order δ:

$$\dot{y} = \delta Q^T F_1(Vx + O(\delta)) + Q^T F_2(\delta Q y_1(x) + O(\delta^2)). \tag{2.40}$$

Since the Jacobian of F_2 in 0 was $B = -I + \mathbb{1}_N/N$, the second term can be expanded as (note that $\mathbb{1}_N Q = 0$)

$$\begin{aligned} Q^T F_2(\delta Q y_1(x) + O(\delta^2)) &= \delta Q^T B Q y_1(x) + O(\delta^2) = -\delta Q^T Q y_1(x) + O(\delta^2) \\ &= -\delta y_1(x) + O(\delta^2). \end{aligned}$$

Thus, (2.40) implies that the first expansion coefficient $y_1(x)$ of the slow manifold equals

$$y_1(x) = Q^T F_1(Vx).$$

The slow manifold $\mathcal{C}_\delta$ has a graph with the expansion

$$y(x, \delta) = \delta Q^T F_1(Vx) + O(\delta^2).$$

Inserting this expansion into the equation for the variable x we see that x is the slow variable:

$$\dot{x} = \delta V^T F_1(Vx + O(\delta)) + V^T F_2(\delta Q Q^T F_1(Vx) + O(\delta^2)).$$

Using again that $\partial F_2(0) = B = -I + \mathbb{1}_N/N$, we see that the terms of order δ in the second term are zero, such that the first-order expansion of the dynamics on the slow manifold is

$$\dot{x} = \delta V^T F_1(Vx) + O(\delta^2). \tag{2.41}$$

This result holds uniformly for all N and subgroup sizes for informed groups. For example, when only two individuals have information (without loss of generality $\bar{\theta}_2 = -\bar{\theta}_1$ of equal conviction($a_1 = a_2 = 1/\sqrt{2}, a_j = 0$ for $j > 2$)), then the slow dynamics is

$$\dot{x} = \frac{\delta}{N\sqrt{2}}\Big[\sin\big(\bar{\theta}_1 - (x + O(\delta)\big) + \sin\big(-\bar{\theta}_1 - (x + O(\delta)\big)\Big]. \tag{2.42}$$

Dropping terms of order δ^2 in this equation and rescaling time by $\delta/(N\sqrt{2})$ gives the approximation

$$\dot{x} = \Big[\sin\big(\bar{\theta}_1 - x\big) + \sin\big(-\bar{\theta}_1 - x\big)\Big] = -2\cos\bar{\theta}_1 \sin x. \tag{2.43}$$

In this first-order approximation the equilibrium $x = 0$ is stable if $|\bar{\theta}_1| < \pi/2$, but unstable if $|\bar{\theta}_1| > \pi/2$. For $|\bar{\theta}_1| > \pi/2$ the equilibrium $x = \pi$ is stable, while for $\bar{\theta}_1 = \pi/2$ all x are equilibria. This degenerate situation is resolved by incorporating $O(\delta^2)$ terms. Section 3 will study this scenario (the case of large coupling coefficient K in its notation) in more detail.

2.4 Perturbation of sinusoidal coupling

The stability of symmetric equilibria depends on the coupling function. For further information about this see Brown et al. [2]. In system (2.1) we have a purely sinusoidal coupling term $\sin(\theta_\ell - \theta_j)$ from angle ℓ to angle j. This is a somewhat degenerate case. In practice this means that the influence of individual j on indi-

vidual ℓ is maximal when their respective orientation is at a right angle. A straight forward and sensible generalization of this coupling is to assume that the influence of another individual is maximal when its orientation angle is at some other optimal value θ_* that is smaller than $\frac{\pi}{2}$, specifically $\theta_* \in (0, \frac{\pi}{2})$, such that a set of plausible mutual coupling functions for the more general system

$$\dot{\theta}_j = a_j \sin\left(\bar{\theta}_j - \theta_j\right) + \frac{1}{N}\sum_{\ell=1}^{N} g(\theta_\ell - \theta_j) \tag{2.44}$$

would be coupling functions g with the properties

1. g is periodic with base period interval $[-\pi, \pi]$,
2. g is odd $\big(g(x) = -g(-x)\big)$,
3. $g(x) > 0$ if $x \in (0, \pi)$,
4. $g(x)$ has a single maximum $\theta_* \in (0, \frac{\pi}{2}]$.

The coupling function $g(x) = \sin x$ has the above properties, with its maximum at $\theta_* = \frac{\pi}{2}$. A more general class of admissible coupling functions would include a second harmonic, such as

$$g_c(x) = \sin x + c\sin(2x) \quad \text{with } c \in [0, 1/2). \tag{2.45}$$

2.4.1 The limit of strong bias

Before showing a numerical example where a group with equal preference is split in a stable equilibrium, we discuss the underlying mechanism. This mechanism is clearest in the limit of strong preferences:

$$a_j = \frac{1}{\epsilon} \gg 1 \quad \text{for all } j = 1, \ldots, N,$$

and applies for arbitrarily small coefficient $c > 0$ of the second harmonic.

We consider a population consisting of two informed groups consisting of an equal number p of individuals and one group of naive individuals consisting of two individuals. The informed groups are heading in opposite directions. The first group has preference angle $\bar{\theta}_1 = -\frac{\pi}{2}$, the second group has preference angle $\bar{\theta}_2 = \frac{\pi}{2}$, and both have preference strengths $a_j = 1/\epsilon$. We assign the indices 1 and 2 for the naive

individuals, and $3, \ldots, p+2$ and $p+3, \ldots, 2p+2$ for the two informed groups. This results in the following system of differential equations

$$\begin{aligned}
\dot{\theta}_j &= \frac{1}{N}\sum_{\ell=1}^{N} g_c(\theta_\ell - \theta_j), \quad \text{for } j = 1, 2, \\
\dot{\theta}_j &= \frac{1}{\epsilon}\sin\Big(-\frac{\pi}{2} - \theta_j\Big) + \frac{1}{N}\sum_{\ell=1}^{N} g_c(\theta_\ell - \theta_j) \\
&=: -\frac{1}{\epsilon}\cos\theta_j + h_j\big(\theta_1, ..., \theta_N, t\big) \quad \text{for } j = 3, ..., p+2, \\
\dot{\theta}_j &= \frac{1}{\epsilon}\sin\Big(\frac{\pi}{2} - \theta_j\Big) + \frac{1}{N}\sum_{\ell=1}^{N} g_c(\theta_\ell - \theta_j) \\
&=: \frac{1}{\epsilon}\cos\theta_j + h_j\big(\theta_1, ..., \theta_N, t\big) \quad \text{for } j = p+3, ..., 2p+2.
\end{aligned} \tag{2.46}$$

Multiplying both sides of the last two equations from (2.46) by ϵ gives

$$\dot{\theta}_j = \frac{1}{N}\sum_{\ell=1}^{N} g_c(\theta_\ell - \theta_j), \quad \text{for } j = 1, 2, \tag{2.47}$$

$$\epsilon\dot{\theta}_j = -\cos\theta_j + \epsilon h_j(\theta_1, ..., \theta_N) \quad \text{for } j = 3, ..., p+2, \tag{2.48}$$

$$\epsilon\dot{\theta}_j = \cos\theta_j + \epsilon h_j\big(\theta_1, ..., \theta_N\big) \quad \text{for } j = p+3, ..., 2p+2. \tag{2.49}$$

According to [13], system (2.47)–(2.49) is in standard form of a slow-fast system that has two time scales (slow and fast) since each of the functions $\cos\theta_j$ and $-\cos\theta_j$ has real isolated roots. To apply the standard theory for singularly perturbed systems we have to first rescale time $\mathrm{d}/\mathrm{d}t_{\text{new}} = \epsilon\,\mathrm{d}/\mathrm{d}t_{\text{old}}$ (we use $(\cdot)'$ for the derivative in the fast time t_{new}):

$$\theta_j' = \epsilon\frac{1}{N}\sum_{\ell=1}^{N} g_c(\theta_\ell - \theta_j), \quad \text{for } j = 1, 2, \tag{2.50}$$

$$\theta_j' = -\cos\theta_j + \epsilon h_j(\theta_1, ..., \theta_N) \quad \text{for } j = 3, ..., p+2, \tag{2.51}$$

$$\theta_j' = \cos\theta_j + \epsilon h_j\big(\theta_1, ..., \theta_N\big) \quad \text{for } j = p+3, ..., 2p+2. \tag{2.52}$$

Next we determine the set of stable equilibria in this fast time at $\epsilon = 0$, when considering the slow variables θ_1 and θ_2 as parameters,

$$\theta_j' = 0, \quad \text{for } j = 1, 2, \tag{2.53}$$

$$\theta_j' = -\cos\theta_j \quad \text{for } j = 3, ..., p+2, \tag{2.54}$$

$$\theta_j' = \cos\theta_j \quad \text{for } j = p+3, ..., 2p+2. \tag{2.55}$$

This gives (for arbitrary θ_1 and θ_2) $\theta_j = -\pi/2$ for $j = 3, \ldots, p+2$ and $\theta_j = \pi/2$ for $j = p+3, \ldots, 2p+2$ as stable equilibria in the fast time. Now we can go back to the slow time and replace in the slow equations (2.47) all variables with their equilibrium values from the fast limit (2.54), (2.55): $\theta_j = -\pi/2$ for $j = 3, \ldots, p+2$ and $\theta_j = \pi/2$ for $j = p+3, \ldots, 2p+2$. The result will be accurate up to terms of order ϵ (note that $N = 2p+2$):

$$\dot{\theta}_1 = \frac{1}{2p+2}\left[g_c(\theta_2 - \theta_1) + pg_c\left(-\frac{\pi}{2} - \theta_1\right) + pg_c\left(\frac{\pi}{2} - \theta_1\right) + O(\epsilon)\right], \tag{2.56}$$

$$\dot{\theta}_2 = \frac{1}{2p+2}\left[g_c(\theta_1 - \theta_2) + pg_c\left(-\frac{\pi}{2} - \theta_2\right) + pg_c\left(\frac{\pi}{2} - \theta_2\right) + O(\epsilon)\right]. \tag{2.57}$$

The above system is the two dimensional slow subsystem of (2.47)–(2.49). We now insert the concrete form of g_c, $g_c(x) = \sin x + c\sin(2x)$, which implies that

$$g_c(0) = g_c(\pi) = g_c(-\pi) = 0, \quad \text{and}$$
$$g_c'(0) = 1 + 2c, \quad g_c'(\pi) = g_c'(-\pi) = -1 + 2c.$$

Furthermore, system (2.47)–(2.49) is symmetric with respect to the permutation $P : (\theta_1, \theta_2) \mapsto (\theta_2, \theta_1)$. Thus, (2.56), (2.57) has the two equilibria $E_0 = (-\frac{\pi}{2} + O(\epsilon), \frac{\pi}{2} + O(\epsilon))$ and $E_1 = (\frac{\pi}{2} + O(\epsilon), -\frac{\pi}{2} + O(\epsilon))$. The equilibria are symmetrically related to each other via permutation P such that they have the same Jacobian J:

$$J = \frac{1}{2p+2}\begin{bmatrix} -4pc + 1 - 2c & -1 + 2c \\ -1 + 2c & -4pc + 1 - 2c \end{bmatrix} + O(\epsilon) \tag{2.58}$$

The Jacobian matrix J of the right-hand side has the eigenvalues $\lambda_1 = -4cp$, $\lambda_2 = 2 - 4c - 4cp$. Both eigenvalues are negative if

$$\frac{1}{2(1+p)} < c.$$

For the coupling function g_c to be admissible we require that $c \in [0, 1/2)$. Hence, if ϵ is sufficiently small and the size of the informed groups, p, is positive, we can find a coefficient c for the second harmonic component of g_c such that g_c is admissible and the equilibria E_0 and E_1 are stable. We can even choose $c > 0$ arbitrarily small, if p is correspondingly large. The resulting stable equilibrium with split naive group has the angles $\theta_1 = -\pi/2 + O(\epsilon)$ and $\theta_2 = \pi/2 + O(\epsilon)$ for the naive individuals. This implies that the group without preference has been split in a stable equilibrium.

2.4.2 Numerical demonstration of a stable splitting

We tested a simulation of the full system (2.44) with coupling function $g(x) = \sin x + 0.3 \sin(2x)$, $p = 5$. The groups are called N_1 and N_2 for informed individuals with preference in opposite directions in the legend of figure 2.2. Group N_3 of size 4 are uninformed individuals ($a_j = 0$). The bias strength was chosen moderately large ($\epsilon = 0.7$). The result of the simulations is in figure 2.2. It shows that the uninformed group splits into two pairs in the equilibrium, both staying close to the one of the informed groups. One group stays slightly above $\pi/2$, the other slightly below $3\pi/2$ (equaling $-\pi/2$ up to 2π).

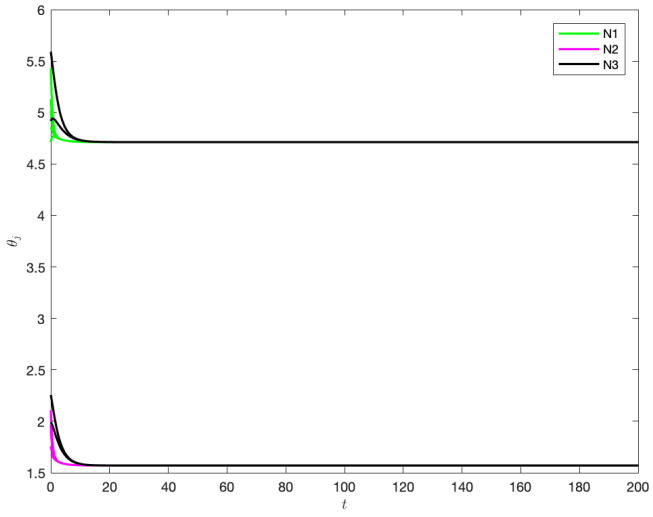

Fig. 2.2 Time profile for system (2.44). N_1: group of individuals preferring $\bar{\theta}_1$, N_2: group of individuals preferring $\bar{\theta}_2$, N_3: uninformed individuals, $\bar{\theta}_1 = -\frac{\pi}{2}, \bar{\theta}_2 = \frac{\pi}{2}$, size of N_1 and N_2 is 5, size of N_3 is 4, other parameters: $c = 0.3$, $\epsilon = 0.7$.

Chapter 3

Competition between two informed groups of equal size

3.1 Introduction

In this part of the thesis we study the case of three groups. We assume that the groups 1 (of size N_1) and 2 (of size N_2) have preferred orientation angles $\bar{\theta}_1$ and $\bar{\theta}_2$, respectively, with equal strength of preference. We also assume that group 3 (of size $N_3 = N - N_1 - N_2$) is uninformed (naive). The oscillators θ_j then follow a system of differential equations of the form

$$\begin{aligned}
\dot{\theta}_j &= \sin(\bar{\theta}_1 - \theta_j) + \frac{K}{N}\sum_{l=1}^{N}\sin(\theta_l - \theta_j), \quad j \in \aleph_1 \\
\dot{\theta}_j &= \sin(\bar{\theta}_2 - \theta_j) + \frac{K}{N}\sum_{l=1}^{N}\sin(\theta_l - \theta_j), \quad j \in \aleph_2 \\
\dot{\theta}_j &= \frac{K}{N}\sum_{l=1}^{N}\sin(\theta_l - \theta_j). \quad j \in \aleph_3.]
\end{aligned} \tag{3.1}$$

We know from section (2.3.2) Lemma (2) that individuals of each group stay together such that we can reduce system (3.1) to a three-dimensional ODE. Following from

(3.1) the group orientations satisfy the equations

$$\begin{aligned}\dot{\psi}_1 &= \sin(\bar{\theta}_1 - \psi_1) + \frac{KN_2}{N}\sin(\psi_2 - \psi_1) + \frac{KN_3}{N}\sin(\psi_3 - \psi_1)\\ \dot{\psi}_2 &= \sin(\bar{\theta}_2 - \psi_2) + \frac{KN_1}{N}\sin(\psi_1 - \psi_2) + \frac{KN_3}{N}\sin(\psi_3 - \psi_2)\\ \dot{\psi}_3 &= \frac{KN_1}{N}\sin(\psi_1 - \psi_3) + \frac{KN_2}{N}\sin(\psi_2 - \psi_3)\end{aligned} \tag{3.2}$$

where the orientations of the respective groups (called ψ_1, ψ_2, ψ_3) are the dependent variables. In this system there are only three parameters:

- the difference between the preference angles $\bar{\theta}_1 - \bar{\theta}_2$,
- the coupling strength K between individuals relative to the preferences (not considered as bifurcation parameter in [16]),
- the ratios between group sizes N_1/N and N_2/N ($N_3 = N - N_1 - N_1$).

We keep our setup symmetric ($N_1 = N_2$) and consider the case where the informed groups are small compared to the naive group (specifically, fixing $N_1/N = N_2/N = 2/9$). This leaves two parameters for our bifurcation analysis, K and $\bar{\theta}_1 - \bar{\theta}_2$. The subsections below will show one-parameter analysis in $\bar{\theta}_1 - \bar{\theta}_2$ for three cases of K: $K \gg 1$ (specifically $K = 30$), $K = 1$ and $K \ll 1$ (specifically $K = 0.2$). We note that the multi-agent system is a gradient system associated with a periodic potential function. This is based on section 2.2 Lemma 1. Thus, we expect to have stable nodes or saddles only. Also, we expect that equilibrium branches repeat every multiple of 2π in each direction, due to the periodicity of the right-hand side of (3.2). The configurations of groups orientations in these equilibria branches are yet to be found from bifurcation diagrams. The bifurcations diagrams shown in the following section have been computed using the COCO package in Matlab on the full system since the results from the reduced system (for ψ) and the full system (for θ_j, $j = 1, \ldots, N$) are identical. The Matlab package is a numerical continuation toolbox [6]. See also [7] for tutorials and user guidance.

3.2 Bifurcation analysis

3.2.1 Strong coupling: large K

For this case, we set K to 30. We started from a stable steady state obtained by simulation at parameter value $\bar{\theta}_1 - \bar{\theta}_2 = -2$. This was followed by using the steady

state as an initial condition to track the equilibria branch. The steady state from numerical simulations gave the middle branch that consists of stable nodes before the branching point(indicated by the colour blue) in figures (3.1a), (3.1b) and (3.1c) The bifurcation diagrams in figure (3.1) show that all ψ_k for stay close to each other

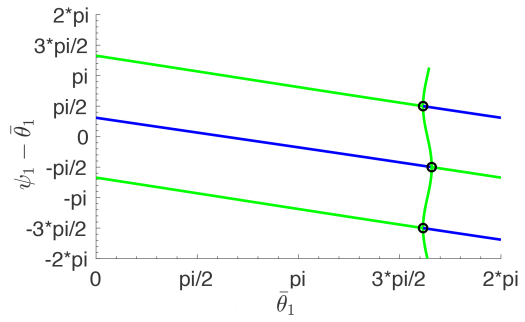

(a) $\bar{\theta}_1$ vs. $\psi_1 - \bar{\theta}_1$

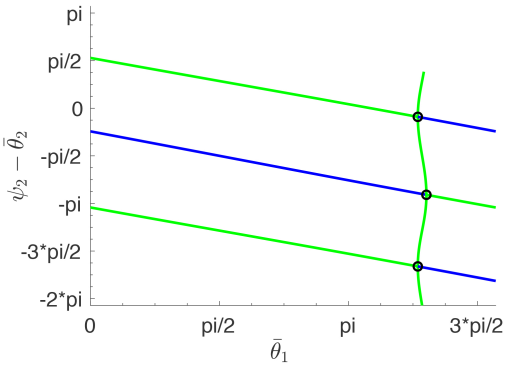

(b) $\bar{\theta}_1$ vs. $\psi_2 - \bar{\theta}_2$

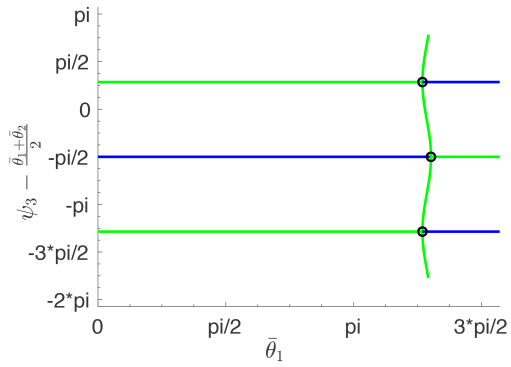

(c) $\bar{\theta}_1$ vs. $\psi_3 - \frac{\bar{\theta}_1 - \bar{\theta}_2}{2}$

Fig. 3.1 Individuals respond to phase difference. $\bar{\theta}_2 = 2$, $N_1 = N_2 = 20$, $N_3 = 50$, $K = 30$, and stability code: blue=stable, green=unstable, black circle=symmetry breaking

for strong coupling K along all branches. The data of the branches recorded by COCO Showed that the blue branches are symmetric whereas the green ones are unsymmetric. In blue branch, we have naive individuals located between informed individuals such that $\psi_3 \neq (\bar{\theta}_1 + \bar{\theta}_2)/2 \mod (2\pi)$. These configurations are illustrated in figures (3.2) and (3.4) where we have configurations of five equilibria. The locations of theses equilibria can be found in figures (3.3) and (3.5).

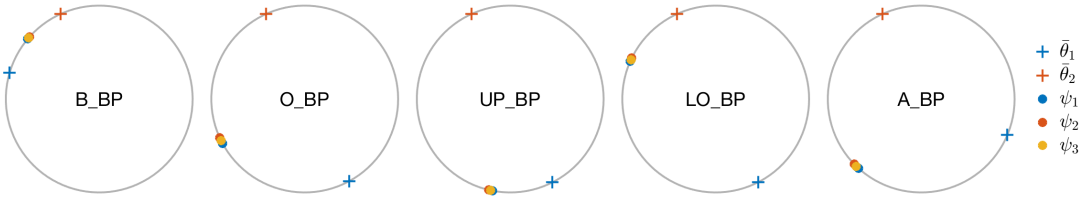

Fig. 3.2 Orientations configurations on branches that connect through middle branching point for $K = 30$.
B_BP=before branching point, UP_BP=upper branch emanating from branching point, LO_BP=lower branch emanating from branching point, A_BP=after branching point

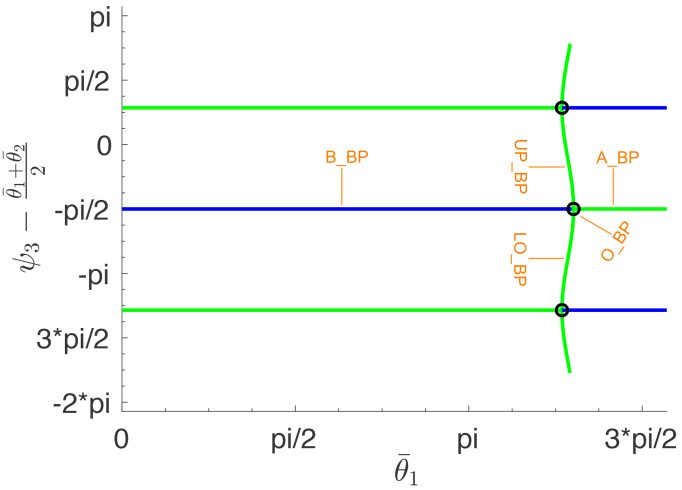

Fig. 3.3 Locations of five equilibria exhibited in first orientations configurations figure for $K = 30$

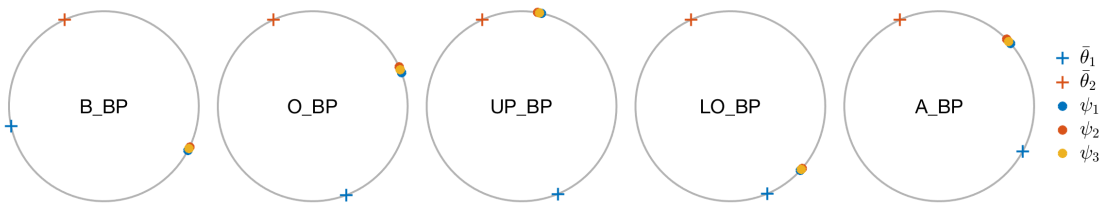

Fig. 3.4 Orientations configurations on branches that connect through upper branching point for $K = 30$.
B_BP=before branching point, UP_BP=upper branch emanating from branching point, LO_BP=lower branch emanating from branching point, A_BP=after branching point

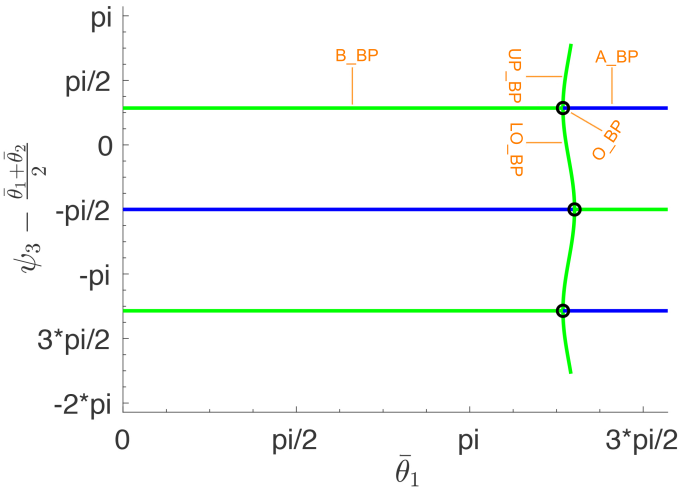

Fig. 3.5 Locations of five equilibria exhibited in second orientations configurations figure for $K = 30$

We note that the configurations of equilibria branches that connect through lower branching point are similar to the configuration illustrated in figure (3.4). This follows from the fact that the potential function associated to the multi-agents system is periodic. There are two different kinds of orientation configurations. In the first type we have all three groups aligned closely together approximately in the middle between $\bar{\theta}_1$ and $\bar{\theta}_2$. In the second type we have all groups aligned closely together in a direction that is the opposite to approximate middle direction between $\bar{\theta}_1$ and $\bar{\theta}_2$. At the branching point, the phase difference $\bar{\theta}_1 - \bar{\theta}_2$ has a value near π, meaning that the preferred direction are nearly opposite to each other. In a scenario of animal groups

the symmetry breaking could be interpreted as an orientation switch of the entire group when the two informed groups have diametrically opposing preferences. With strong coupling the group stays together even along the unsymmetric branch, as illustrated in the circles labelled with "UP_BP" and "LO_BP" in figures (3.2) and (3.4), and, according to simulations, also dynamically. The symmetry breaking is subcritical. This can be intuitively explained by the observation that, for $\bar{\theta}_1 = \bar{\theta}_2 + \pi$ (diametrically opposing preferences), one symmetric state with $\psi_3 = (\bar{\theta}_1 + \bar{\theta}_2)/2$ mod (2π) and $\psi_1 - \psi_3 = -(\psi_2 - \psi_3)$ is still stable. Consequently, its mirror image, with $\psi_j \mapsto -\psi_j$ must also be stable, implying subcriticality of the symmetry breaking and instability of the unsymmetric branch. Past the branching point, the phase difference $\overline{\theta}_1 - \overline{\theta}_2$ starts to decrease again(modulo 2π) such that the orientations configurations in the branches are mirror images of the case for $\bar{\theta}_1 - \bar{\theta}_2 \in (0, \pi)$. This can be observed in circles labelled with "A_BP" in figures (3.2) and (3.4). These circles also indicate that branches swapped configurations. In general, we can say that the large coupling coefficient causes the population to remain closely together. For large K there is a small region of bistability near the parameter region where the informed groups have diametrically opposite preferences. In this region the stable state chosen by the system depends on the initial conditions.

3.2.2 Second Case:Intermediate-strength coupling $K = 1$

In the previous case the coupling force was dominant, and all three groups choose to stick closely together. For the current case we want to see what kind of configurations we get if we choose K such that the coupling force is not as strong as the previous case, yet not very weak. Thus, we set $K = 1$. Tracking equilibria branches for this choice of K gave the the branches in figure (3.6)

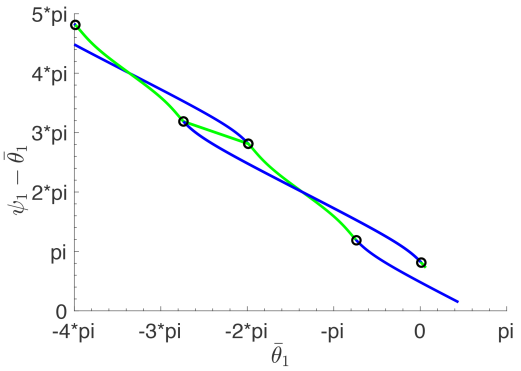

(a) $\bar{\theta}_1$ vs. $\psi_2 - \bar{\theta}_2$

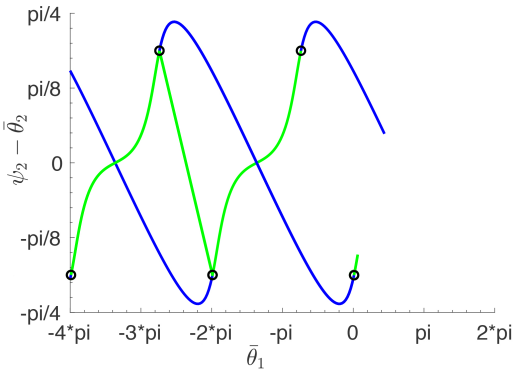

(b) $\bar{\theta}_1$ vs. $\psi_2 - \bar{\theta}_2$

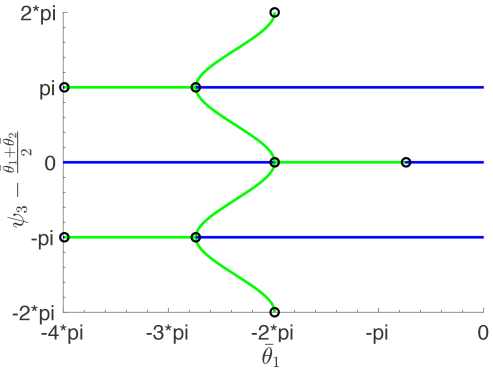

(c) $\bar{\theta}_1$ vs. $\psi_3 - \frac{\bar{\theta}_1-\bar{\theta}_2}{2}$

Fig. 3.6 Population groups correspondence to phase difference with $K = 1$

For intermediate-strength coupling ($K = 1$) the bifurcation diagram, shown in figure (3.6), is qualitatively the same as for strong coupling that was in the settings of figures shown in (3.1). However, we observe a stronger alignment of the informed groups with their preferred directions:$|\psi_1 - \bar{\theta}_1|$ and $|\psi_2 - \bar{\theta}_2|$ are always less than $\pi/3$. We observe that the behaviour of naive group is nearly identical to the large coupling case: in the symmetric configurations $\psi_3 = (\bar{\theta}_1 + \bar{\theta}_2)/2 \mod (2\pi)$. However, the informed groups have qualitatively different non-symmetric branches. While for large K the non-symmetric branch covers the full circle for the quantity $\psi_j - \bar{\theta}_j$ (for $j = 1, 2$), this is no longer the case for $K = 1$. Both parts of non-symmetric branch are bounded (and identical) in ψ_2, see figure (3.6b). The informed do no longer stay close to the naive group, but stay close to their preferred direction along the non-symmetric branch. We observe that branching points appear when $\bar{\theta}_1 - \bar{\theta}_2$ is equal to 0.0368 or 3.9633 where the branches lose their stability. We Also observe that the region where two stable states coexist is larger for intermediate K than for large

K. For detailed information about orientations configurations details see figures (3.7) and (3.9)

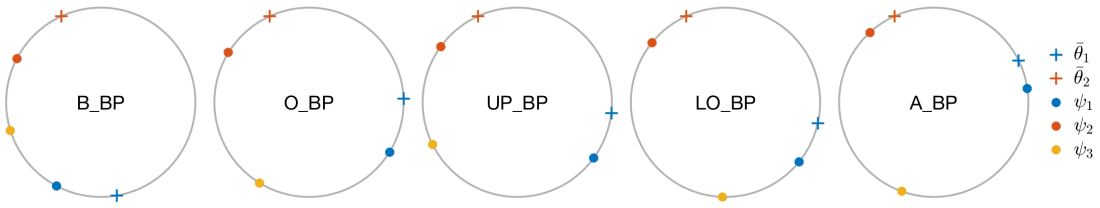

Fig. 3.7 Orientations configurations on branches that connect through middle branching point for $K = 1$.
B_BP=before branching point, UP_BP=upper branch emanating from branching point, LO_BP=lower branch emanating from branching point, A_BP=after branching point

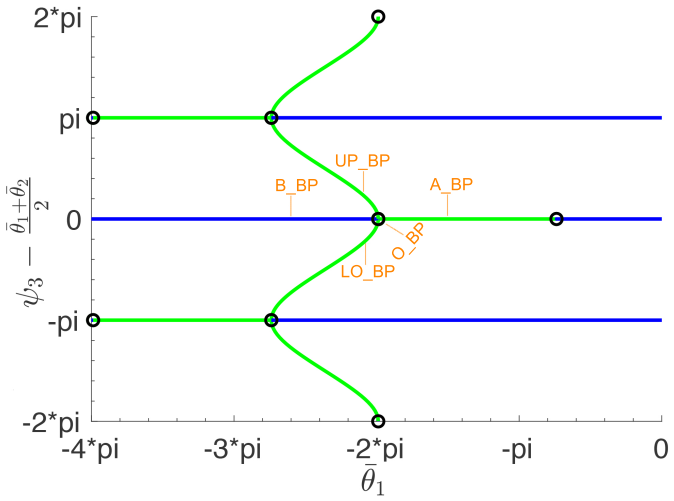

Fig. 3.8 Locations of five equilibria exhibited in first orientations configurations figure for $K = 1$

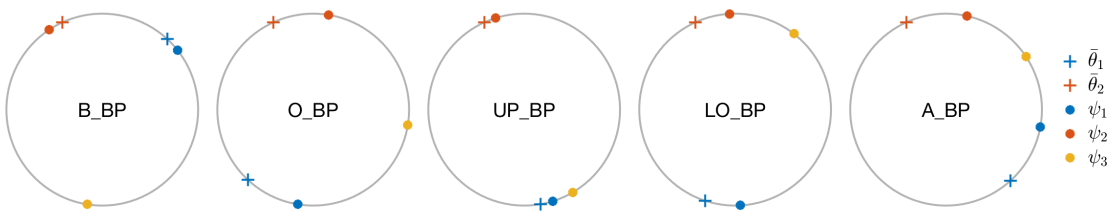

Fig. 3.9 Orientations configurations on branches that connect through upper branching point for $K = 1$.
B_BP=before branching point, UP_BP=upper branch emanating from branching point, LO_BP=lower branch emanating from branching point, A_BP=after branching point

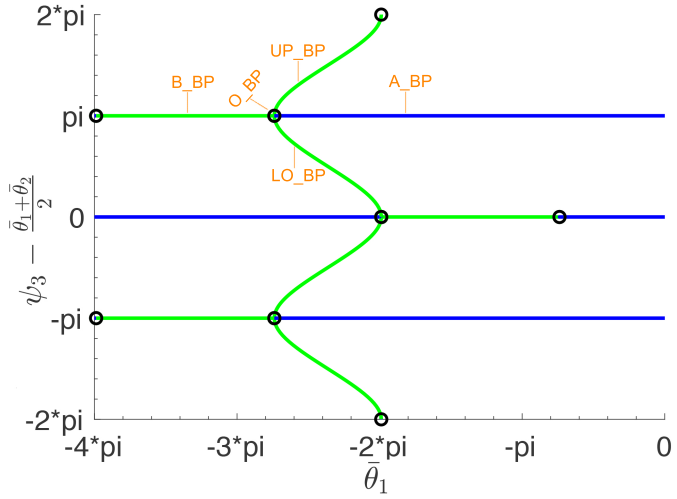

Fig. 3.10 Locations of five equilibria exhibited in second orientations configurations figure for $K = 1$

The orientations configurations illustrated in figures (3.7) and (3.9) indicate that all three groups are trying to stick closely together but not as close as the previous case since the coupling force is a lot weaker. We observe that the configuration on the upper and lower branches emanating from the branching point are similar to the previous case of strong coupling $K = 30$(naive individuals choose to approach one of the informed groups). The non-symmetric branch connects the symmetric branch with its mirror image $\psi_j \mapsto -\psi_j$. In the last case for $K = 30$ the branching point appeared when $\bar{\theta}_1 - \bar{\theta}_2$ is close to π, but in this case we have the branching occurring

when $\bar{\theta}_1 - \bar{\theta}_2$ is close to π, also when it's close to 4. As a result, we have a longer region of bistability comparing to the last case when $K = 30$. We observed when comparing between figures (3.1b) and (3.6b) that we don't have three unsymmetric branches connected through branching points, the curve tracking details indicated that the third line is identical to the straight tilted green line and located underneath it.

3.2.3 Third Case:Small coupling limit $K = 0.2$

In this section we study the case of weak coupling and find its pitchfork (symmetry-breaking) bifurcations. Thus, we set the coupling coefficient to $K = 0.2$. Tracking equilibria branches for this choice of coupling coefficient gave the results shown in figure (3.11)

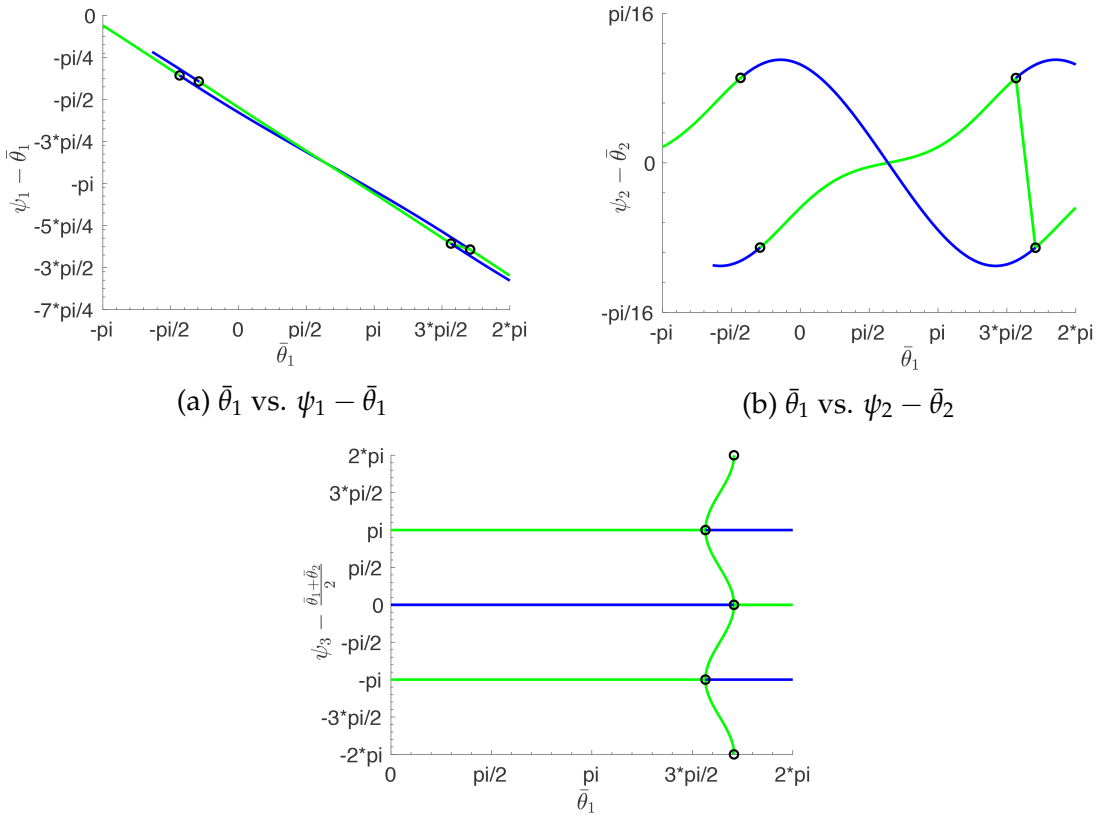

(a) $\bar{\theta}_1$ vs. $\psi_1 - \bar{\theta}_1$

(b) $\bar{\theta}_1$ vs. $\psi_2 - \bar{\theta}_2$

(c) $\bar{\theta}_1$ vs. $\psi_3 - \frac{\bar{\theta}_1 - \bar{\theta}_2}{2}$

Fig. 3.11 Population groups correspondence to phase difference with $K = 0.2$

We observe that bifurcation diagrams in figure (3.11) indicate that informed individuals have stronger tendency than the cases of intermediate and small K to

follow their preferred directions. The naive individuals behaviour is similar to the previous cases, they choose a heading direction between the preferred directions of informed individuals. The branching occurs where $\bar{\theta}_1 - \bar{\theta}_2$ is approximately equal to π. We observe that the bistabilitly region shrinks again. Detailed information about orientations configuration are in figures (3.12) and (3.14)

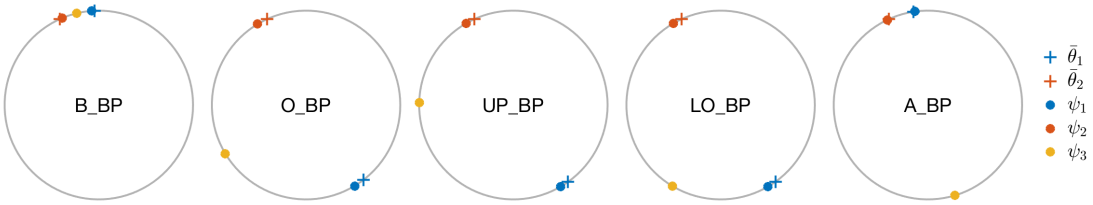

Fig. 3.12 Orientations configurations on branches that connect through middle branching point for $K = 0.2$.
B_BP=before branching point, UP_BP=upper branch emanating from branching point, LO_BP=lower branch emanating from branching point, A_BP=after branching point

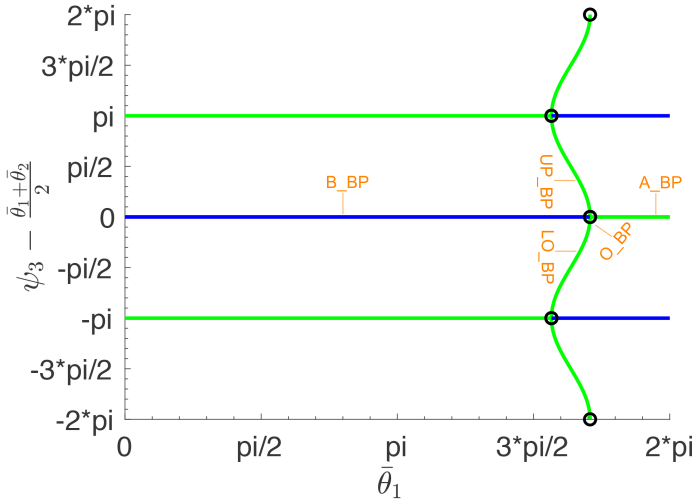

Fig. 3.13 Locations of five equilibria exhibited in first orientations configurations figure for $K = 0.2$

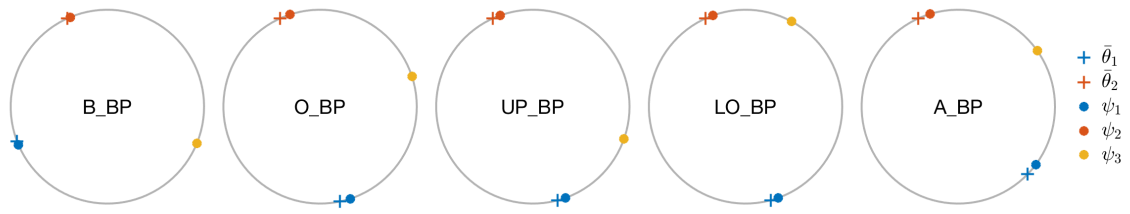

Fig. 3.14 Orientations configurations on branches that connect through upper branching point for $K = 0.2$.
B_BP=before branching point, UP_BP=upper branch emanating from branching point, LO_BP=lower branch emanating from branching point, A_BP=after branching point

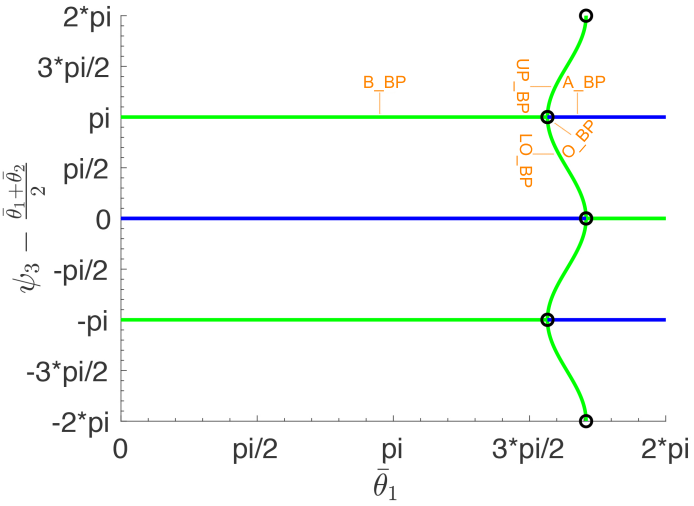

Fig. 3.15 Locations of five equilibria exhibited in second orientations configurations figure for $K = 0.2$

The orientation configurations indicate that informed individuals have a stronger tendency to follow their preferred direction. This can be seen from the phase difference between informed individuals and their preferred directions that is smaller than the cases of strong coupling and intermediate coupling.

Chapter 4

Interpretation and Conclusions

4.1 Interpretation of results

As explained at the beginning of Chapter 3, our general Theorem 1 justifies the consideration of reduced models such as (3.2). Individuals with the same preference must almost surely align asymptotically (at least when the coupling is sinusoidal). This permits one to consider large swarms as a collection of a small number of groups, weighted by their size. While the theorem is valid only for purely sinusoidal coupling, realistic coupling functions will be close to sinusoidal. Our construction of a scenario with splitting when the coupling is not sinusoidal shows that splitting requires large informed groups with diametrically opposed preferences. Thus, splitting for groups with identical preference will be unlikely to occur in large parameter regions in more complex models. This suggests that more complex models may be reducible to group models too.

Our numerical bifurcation analysis shows that the degree of alignment increases monotonically with the coupling strength (and decreases with the strength of preferences). This may make it possible to infer these parameters from field observations or experiments. Our numerical analysis also showed that in the two parameter plane no stable steady states with broken reflection symmetry exist (where, for example, the uninformed group aligns more with either one of the informed groups. instead we found that all such unsymmetric states are unstable. This results in bistability between the two different possible symmetric states around the parameters where symmetry breaking occurs (when the informed groups have diametrically opposing preferences). Consequently, for scenarios where symmetry breaking occurs other effects beyond the orientation balance between alignment and preference may have to be considered.

4.2 Conclusions

In all three cases of coupling force strength we observed two types of configurations. The first one is when all three groups are aligned in the the shorter arc in reference to the preferred directions(Configurations in symmetric branches). The second one is when all three individuals are aligned in the longer arc(Configurations in unsymmetric branches). We observed three phenomena that resulted from changing the magnitude of coupling coefficient K. The first observation is the the phase difference between groups. It decreases as we increase K. The second observation is the bistability region. For large K, no bistability region was detected. For intermediate and small K, bistability region was detected such that for intermediate K it was much more noticeable than small K. We believe that the bistability region for intermediate K is larger than all other K values because the bias force is competing with coupling force(none of the force weigh more than the other one). The third observation is the length of the shorter arc in the circle . It increases and then switch to a different side of the circle for large and small K, whereas for intermediate K the shorter arc preserves its length and switch to the other side of circle. So far we investigated the possible configurations for the mathematical model with the coupling force that was found in the original literature [21]. We believe that if the coupling force was replaced by the one introduced in the last section of chapter two, we would have different configurations since the slow manifold is two dimensional.

References

[1] Acebrón, J. A., Bonilla, L. L., Vicente, C. J. P., Ritort, F., and Spigler, R. (2005). The Kuramoto model: A simple paradigm for synchronization phenomena. *Reviews of modern physics*, 77(1):137.

[2] Brown, E., Holmes, P., and Moehlis, J. (2003). Globally coupled oscillator networks. In *Perspectives and Problems in Nolinear Science*, pages 183–215. Springer.

[3] Chan, N. and Li, K.-H. (1983). Diagonal elements and eigenvalues of a real symmetric matrix. *Journal of Mathematical Analysis and Applications*, 91(2):562–566.

[4] Couzin, I. D. and Franks, N. R. (2003). Self-organized lane formation and optimized traffic flow in army ants. *Proceedings of the Royal Society of London. Series B: Biological Sciences*, 270(1511):139–146.

[5] Couzin, I. D., Krause, J., Franks, N. R., and Levin, S. A. (2005). Effective leadership and decision-making in animal groups on the move. *Nature*, 433(7025):513.

[6] Dankowicz, H. and Schilder, F. (2013). *Recipes for continuation*. Society for Industrial and Applied Mathematics, Philadelphia.

[7] Dankowicz, H. and Schilder, F. (2015). The equilibrium point toolbox.

[8] Ermentrout, B. (1991). An adaptive model for synchrony in the firefly pteroptyx malaccae. *Journal of Mathematical Biology*, 29(6):571–585.

[9] Gharan, S. O. (2016). Design and analysis of algorithms I.

[10] Hirsch, M. W., Smale, S., and Devaney, R. L. (2013). *Differential equations, dynamical systems, and an introduction to chaos*. Elsevier, Academic Press, Amsterdam.

[11] Hoare, D. J., Couzin, I. D., Godin, J.-G., and Krause, J. (2004). Context-dependent group size choice in fish. *Animal Behaviour*, 67(1):155–164.

[12] Jadbabaie, A., Motee, N., and Barahona, M. (2004). On the stability of the Kuramoto model of coupled nonlinear oscillators. In *American Control Conference, 2004. Proceedings of the 2004*, volume 5, pages 4296–4301. IEEE.

[13] Khalil, H. K. (2014). *Nonlinear systems*. Prentice Hall, Upper Saddle River, NJ.

[14] Kuramoto, Y. (2003). *Chemical oscillations, waves, and turbulence*. Dover Publ., Mineola, NY.

[15] Lay, D. C. (2016). Linear algebra and its applications.

[16] Leonard, N. E., Shen, T., Nabet, B., Scardovi, L., Couzin, I. D., and Levin, S. A. (2012). Decision versus compromise for animal groups in motion. *Proceedings of the National Academy of Sciences*, 109(1):227–232.

[17] Mirollo, R. E. and Strogatz, S. H. (1990). Jump bifurcation and hysteresis in an infinite-dimensional dynamical system of coupled spins. *SIAM Journal on Applied Mathematics*, 50(1):108–124.

[18] Mirollo, R. E. and Strogatz, S. H. (2005). The spectrum of the locked state for the Kuramoto model of coupled oscillators. *Physica D: Nonlinear Phenomena*, 205(1-4):249–266.

[19] Nabet, B. (1996). *Dynamics and Control in Natural and Engineered Multi-Agent Systems*. PhD thesis, New Jersey.

[20] Nabet, B., Leonard, N. E., Couzin, I. D., and Levin, S. A. (2006). Leadership in animal group motion: A bifurcation analysis. In *Proceedings of the 17th International Symposium on Mathematical Theory of Networks and Systems, Kyoto, Japan*, pages 1–14.

[21] Nabet, B., Leonard, N. E., Couzin, I. D., and Levin, S. A. (2009). Dynamics of decision making in animal group motion. *Journal of Nonlinear Science*, 19:399–435.

[22] Strogatz, S. H. (2000). From Kuramoto to Crawford: exploring the onset of synchronization in populations of coupled oscillators. *Physica D: Nonlinear Phenomena*, 143(1-4):1–20.

[23] Strogatz, S. H., Abrams, D. M., McRobie, A., Eckhardt, B., and Ott, E. (2005). Theoretical mechanics: Crowd synchrony on the millennium bridge. *Nature*, 438(7064):43.

[24] Tass, P. A. (2003). A model of desynchronizing deep brain stimulation with a demand-controlled coordinated reset of neural subpopulations. *Biological cybernetics*, 89(2):81–88.

[25] Zhang, X.-D. (2017). *Matrix analysis and applications*. Cambridge University Press.